

# HyDelta

## **WP1E – Impact of high speed hydrogen flow on system integrity and noise**

### D1E.1 – WP1E Report

Status: final

Dit project is medegefinancierd door TKI Nieuw Gas | Topsector Energie uit de PPS-toeslag onder referentienummer TKI2020-HyDelta.

## Document summary

### Corresponding author

Corresponding author	Néstor González Díez
Affiliation	TNO
Email address	nestor.gonzalezdiez@tno.nl

### Document history

Version	Date	Author	Affiliation	Summary of main changes
0.1	14-Aug-2021	N. González Díez, L. van Lier, S. Belfroid, I. Meijer.	TNO	(English) Version for review by WP1E Expert Assessment Group
0.2	3-Nov-2021	(see above)	TNO	(English) Second draft after first review by WP1E Expert Assessment Group. Major modifications implemented in report.
1.0	30-Nov-2021	(see above)	TNO	Final draft submitted for approval to release and translate.

### Dissemination level

Dissemination Level		
<b>PU</b>	Public	x
<b>R1</b>	Restricted to <ul style="list-style-type: none"> <li>Partners including Expert Assessment Group</li> <li>Other project participants including Sounding Board</li> <li>External entity specified by the consortium (please specify)</li> </ul>	
<b>R2</b>	Restricted to <ul style="list-style-type: none"> <li>Partners including Expert Assessment Group</li> <li>Other project participants including Sounding Board</li> </ul>	
<b>R3</b>	Restricted to <ul style="list-style-type: none"> <li>Partners including Expert Assessment Group</li> </ul>	

### Document review

Version	Reviewer name	Affiliation
0.1	Stefan Belfroid Sytze Buruma Thijs Duisters Alfons Krom Gilles de Kok Vinay Sewbaran Johannes de Bruin Pascal te Morsche Peter Verstegen HyDelta Supervisory Group	TNO Coteq Enexis Gasunie Enduris Stedin Liander Liander Liander NEC, KIWA, DNV, TNO, NBNL, Stedin, Alliander
0.2	Sytze Buruma Thijs Duisters Tjidsger Kingma Tessa Hillen Peter Verstegen Rick den Hartog HyDelta Supervisory Group	Coteq Enexis Gasunie Stedin Liander Westland Infra NEC, KIWA, DNV, TNO, NBNL, Stedin, Alliander

## Executive summary

The Netherlands has an extensive pipeline infrastructure for the transport and storage of natural gas. This existing infrastructure could be used in the future for hydrogen transport. For reasons of personal and environmental safety and to ensure reliable supply, the infrastructure is built and operated according to standards and norms for pipeline integrity. Currently, the reliability is ensured by complying with design codes and standards and by using systematic approaches for maintenance and trouble-shooting. The question arises whether the same amount of energy transported with hydrogen as currently with natural gas results in a larger impact on the integrity of the system and the environment around it.

High flow velocities are associated to larger pressure drop and higher risk of noise emissions, vibrations and erosion. The flow speed is determined by the selection of system capacity, operating conditions, hardware sizing and economic evaluation. The combination that provides the lowest levelized cost of transport determines what the resulting flow velocity is at all points of the transport system. However, the flow velocity itself can be a constraint in this optimization due to the risks mentioned. For natural gas, this limit is commonly set at 20 m/s (72 km/h), though this is not the case for every segment of the network and at specific locations this can reach higher values. If the same limit would be applied to hydrogen, it may be an unnecessarily conservative constraint on the capacity of new and re-used systems to transport energy.

In this study, a review is made of flow-induced risk mechanisms for intrusive equipment, flow-induced turbulence, flow-induced pulsations, acoustics-induced vibration, flow-induced noise and erosion. Capacity from a pressure drop perspective is also checked. This is done scoping the Dutch high-pressure gas transport system (GTS), through the RNB systems, up to the gas receiving spot for the end user. A generic benchmark between natural (G-) gas and hydrogen is presented, when an equal energy transport capacity between the two carriers is assumed, which in practice means whether hydrogen can flow 3 times faster than natural gas. The objective of the benchmark is to evaluate whether under this assumption, any of the phenomena analysed hinders transport at such conditions. In other words, whether the allowable flow velocity for hydrogen can be larger than the value traditionally used for natural gas.

Not all of the risks investigated are as prevalent in different segments of the Dutch gas transport and distribution system. Normally, risks associated to vibration and failure are more prevalent in the GTS systems because of the high pressure, whereas the risk of noise is more prevalent with RNB systems. Of course, that does not mean that RNB is insensitive to fatigue failures or GTS to noise-related risks. The table displayed in the next page maps the aforementioned risks to the segment of the Dutch gas network to which they apply.

The main result of this investigation is that the risk levels associated to these phenomena when hydrogen flows with the same energy rate as natural (G-) gas is the same as nowadays. In other words: if with natural gas transport, 20 m/s is a rule of thumb for the maximum flow velocity in the network, 60 m/s can be the rule of thumb for hydrogen, with some caveats as described below. The pipelines have the capacity to operate at 60 m/s from a pressure drop perspective. This means that in exploratory studies for hydrogen network development, capacities of the pipelines to transport hydrogen can be constrained at higher flow velocities than currently done. Applying 20 m/s as for natural gas can be considered conservative.

Table. Fundamental aspects related to flows at high speeds and connection to the different segments of the gas transport and distribution system (indicated by an “x” symbol). For clarification, please refer to section 1.4.

Segment of Gas System	Pressure drop	FIV Intrusive Equipment	Flow Induced Turbulence	Flow Induced Pulsations	Acoustics Induced Vibration	Flow Induced Noise	Erosion
HTL pipeline	x						x
HTL compressor station	x	x	x	x	x	x	x
HTL storage station	x	x	x	x	x	x	x
HTL M&R station	x	x	x	x	x	x	x
HTL GOS	x	x	x	x	x	x	x
RTL pipelines	x						x
RTL GOS	x	x	x	x	x	x	x
RNB pipelines HP	x	x				x	x
RNB pipelines LP	x	x				x	x
RNB gas transfer stations	x	x	x		x	x	x
RNB gas district stations	x	x	x		x	x	x
RNB up to household meter	x		x			x	x

More specifically for the different segments of the gas transport and distribution system, the outcomes of the benchmark between natural gas and hydrogen when transporting the same amount of energy are summarized in the tables displayed in the following pages. A priority number between 1 and 3 has been given based on the level of perceived risk for each mechanism: “1” is given to issues where uncertainties still remain and further research is required; “2” means that the risk perceived is similar (occasionally larger, occasionally lower) for hydrogen as for natural gas, existing engineering practices are valid and should be used when surveying equipment for hydrogen re-use; “3” means that the perceived risk is lower, or in both cases negligible, with hydrogen than with natural gas, existing engineering practices are valid and should be used when surveying equipment for hydrogen re-use.

For the GTS system (HTL, RTL):

Mechanism	Conclusions of benchmark between G-gas and H <sub>2</sub>	Priority
Pressure drop	Similar pressure drop, i.e. pipelines have sufficient capacity to transport the same amount of energy at similar pressure profiles.	3
FIV intrusive equipment	Long, straight designs are at risk if exposed to elevated hydrogen flow speeds. In the examples analysed, some thermowells should be replaced above 38 m/s. Thermowells should be surveyed when re-use service for hydrogen is intended. Existing risk quantification and mitigation measures remain valid. No further research is required.	2
Flow-induced turbulence	Vibrational excitation due to flow-induced turbulence is expected to be more benign with hydrogen even at high flow velocities. Typical supporting layouts should remain sufficient to arrest excitations arising from flow turbulence generated at fittings.	3
Flow-induced pulsations	Flow-induced pulsations are expected to remain a risk similar to current operation with natural gas. While pulsation levels are expected to decrease, their frequency will increase, making them more likely to coincide with mechanical natural frequencies. Analyses as performed nowadays for natural gas will remain the norm for hydrogen service. Existing risk quantification and mitigation measures remain valid and should be applied. No further research is required.	2
Acoustics-induced vibration	Acoustics-induced vibration as the result of depressurization events or pressure reduction in control streets or recycle valves will be more energetic with hydrogen. This is more noticeable the higher the pressure and the diameter of the vent system, for instance on pressure relief on the discharge of compressors. However, this energetic source is unlikely to translate effectively into a higher risk of failure, due to larger distance between acoustic and pipe structural natural frequencies. Installations featuring sudden pressure reduction intended for hydrogen re-use should be surveyed for AIV risk. Existing risk quantification and mitigation measures remain valid and should be applied. No further research is required.	2
Flow-induced noise	Consistently, the noise levels <i>inside</i> the pipe are expected larger for hydrogen than for natural gas. However, the radiation properties of existing pipes tend to block hydrogen noise more (impedance mismatch) than with natural gas. Noise frequencies will increase significantly. It is not possible to conclude that the net effect on <i>external</i> noise emissions is favourable to hydrogen in all cases. It is recommended to continue research by gathering additional experimental evidence on noise emissions from flowing tests and pilot field operations.	2
Erosion	As a result of high flow velocities, erosion potential is dramatically increased. However, measures are in place to prevent the presence of solid particles. Should the amount of solid particles be close to the current legally acceptable limit, flow velocity limits should be applied. Presence of solid particles cannot always be excluded. Existing risk quantification and mitigation measures remain valid. It is recommended to continue the research in the area of erosion (see notes on follow-up recommended research).	1

For the RNB systems (both HP and LP segments):

Mechanism	Conclusions of benchmark between G-gas and H <sub>2</sub>	Priority
Pressure drop	Similar pressure drop, i.e. pipelines have sufficient capacity to transport the same amount of energy at similar pressure profiles. Only small differences are observed depending on the line size or the (inner) surface quality after years of operation.	3
FIV intrusive equipment	Long, straight designs are at risk if exposed to elevated hydrogen flow speeds. In the examples analysed, some thermowells should be replaced above 28 m/s. Thermowells should be surveyed when re-use service for hydrogen is intended. Existing risk quantification and mitigation measures remain valid. No further research is required.	2
Flow-induced turbulence	Vibrational excitation due to flow-induced turbulence is expected to be more benign with hydrogen even at high flow velocities. Typical supporting layouts should remain sufficient to arrest excitations arising from flow turbulence generated at fittings.	3
Acoustics-induced vibration	Acoustics-induced vibration as the result of depressurization events or pressure reduction in control streets or recycle valves will be more energetic with hydrogen. This is more noticeable the higher the pressure and the diameter of the system, for instance in district stations. However, this energetic source is unlikely to translate effectively into a higher risk of failure, due to larger distance between acoustic and pipe structural natural frequencies. Installations featuring sudden pressure reduction intended for hydrogen re-use should be surveyed for AIV risk. Existing risk quantification and mitigation measures remain valid and should be applied. No further research is required.	3
Flow-induced noise	Consistently, the noise levels <i>inside</i> the pipe are expected larger for hydrogen than for natural gas. This is more noticeable the higher the pressure and the diameter of the system, for instance in district stations. However, the radiation properties of existing pipes tend to block hydrogen noise more (impedance mismatch) than with natural gas. Noise frequencies will increase significantly. It is not possible to conclude that the net effect on <i>external</i> noise emissions is favourable to hydrogen in all cases, either in the networks or by the end-user installations such as household. It is recommended to continue research by gathering additional experimental evidence on noise emissions from flowing tests and pilot field operations, including the household level.	2
Erosion	As a result of high flow velocities, erosion potential is expected to increase. However, this is not the result attained for some of the examples used. Several aspects impair the use of existing risk quantification approaches. The results remain uncertain. It is recommended to continue the research in the area of erosion (see follow-up section on recommended research).	1

In terms of follow-up research, the following points are recommended:

- Erosion appears to be the most uncertain mechanism that may prevent achieving the desired flow velocity. In general, flowing hydrogen at high speed (~60 m/s) should translate into an erosion potential of an order of magnitude larger compared to flowing natural gas (at 20 m/s). An important parameter is the level of solid particle contamination in the gas stream, which is uncertain. Filters are in place to prevent this contamination. Assuming legally acceptable limits would already render unacceptable levels of erosion. For RNB systems, the use of the (widely accepted) erosion model is not possible due to the low density of the fluid. Also the characterization of the pipe materials such as PVC is uncertain. It is recommended to investigate this aspect as follows:
  - Exploring the performance of filters in the GTS and RNB systems with high speed hydrogen flow. This should enable a more educated choice for the solid loading in the gas stream.
  - Perform dedicated flow simulations to characterize worst-case erosion rates in the RNB systems, in combination with suitable material constants for PVC pipes, for which tests may be required.
- High frequency dynamic phenomena such as AIV and consequent noise radiation are complex subjects under current investigation even at fundamental levels. Existing engineering practices should be applied to equipment involved in sudden pressure reductions, such as relief valves, compressor recycle valves or flow control valves. This will already limit the risks of AIV sufficiently. To further verify the conclusions obtained in this report about AIV and noise radiation, it is recommended to collect results from tests and actual hydrogen piloting locations conducted in the context of HyDelta and/or its partners.
- Possible metering errors in flow meters as a result of unsteady flows (pulsations, turbulence) should be better understood. This has not been covered in the current scope of HyDelta. It is recommended to explore these phenomena as an integral part of the investigations conducted to determine the requirements for flow metering equipment for hydrogen service.

## Table of contents

Document summary .....	2
Executive summary .....	3
Table of contents .....	8
Nomenclature.....	10
1 Introduction.....	12
1.1 Relevance .....	12
1.2 Scope of Work .....	12
1.3 Earlier and parallel research.....	13
1.4 Gas Transport System.....	14
1.5 Description of the report.....	16
2 Hydrogen Transport .....	17
2.1 Energy Transport Capacity .....	17
2.2 Flow velocity ratio .....	19
2.3 Pressure drop .....	20
2.3.1 Hydrogen vs G-gas.....	20
3 Intrusive Equipment .....	24
3.1 Intrusive equipment in natural gas transport systems .....	24
3.2 Assessment of flow-induced vibration for thermowells .....	24
3.3 Benchmark between natural gas and hydrogen .....	25
3.4 Examples.....	25
3.5 Conclusion .....	25
4 Flow Induced Turbulence .....	26
4.1 Flow Induced Turbulence in natural gas transport systems .....	26
4.2 Assessment of flow-induced turbulence.....	26
4.3 Benchmark between natural gas and hydrogen .....	26
4.4 Examples.....	27
4.5 Conclusion .....	27
5 Flow Induced Pulsations.....	28
5.1 Flow induced pulsations in natural gas transport systems .....	28
5.2 Assessment of flow-induced pulsations.....	28
5.3 Benchmark between natural gas and hydrogen .....	29
5.3.1 Pulsation resonances.....	29
5.3.2 Pulsation amplitudes.....	31
5.4 Examples.....	32

5.4.1	Case with natural gas .....	32
5.4.2	Case with hydrogen .....	32
5.5	Conclusion .....	32
6	Acoustics Induced Vibration .....	34
6.1	Acoustics-Induced Vibration in natural gas transport systems .....	34
6.2	Assessment of Acoustics-Induced Vibration .....	34
6.3	Benchmark between natural gas and hydrogen .....	35
6.4	Examples.....	36
6.5	Conclusion .....	37
7	Flow Induced Noise .....	38
7.1	Flow induced noise in natural gas transport systems .....	38
7.2	Assessment of flow-induced noise.....	39
7.2.1	Source: pressure reduction devices .....	39
7.2.2	Source: pipes and flow fittings .....	39
7.2.3	Radiation.....	40
7.3	Benchmark between natural gas and hydrogen .....	41
7.3.1	Source: pressure reduction devices .....	41
7.3.2	Source: pipe and flow fittings.....	47
7.3.3	Noise radiation .....	47
7.4	Conclusion .....	49
8	Erosion.....	50
8.1	Erosion in natural gas transport systems .....	50
8.2	Assessment of erosion.....	50
8.3	Benchmark between natural gas and hydrogen .....	51
8.4	Examples.....	52
8.5	Conclusion .....	53
9	Perspectives and closing remarks .....	54
10	List of References .....	56

## Nomenclature

### Acronyms

AIV	Acoustics Induced Vibration
AVIFF	Avoidance of Vibration Induced Fatigue Failure
FIP	Flow Induced Pulsations
FIT	Flow Induced Turbulence
Fv	Flow-Induced Vibration Factor
FVF	Fluid Viscosity Factor
GOS	<i>Gasontvangstation</i>
GTS	Gas Transport System
HDPE	High density polyethylene
HHV	High Heating Value [MJ/kg]
HTL	<i>Hoofdtransportleidingnet</i>
HP	High Pressure
LHV	Low Heating Value [MJ/kg]
LP	Low Pressure
LoF	Likelihood of Failure
M&R	<i>Meet- en regelstation</i>
PVC	Polyvinyl Chloride
PWL	Power level [dB]
RNB	Regionale netbeheerders
RTL	<i>Regionale transportleidingnet</i>
SFF	Sonic Flow Factor
WP	Work Package

### Latin symbols

$A$	Frequency-dependent attenuation function [dB]
$C_D$	Discharge coefficient [-]
$c$	Speed of sound [m/s]
$d$	Diameter [m]
$E$	Erosion rate [kg/s]
$f_D$	Darcy friction factor [-]
$f$	Frequency [Hz]
$F$	Dimensionless source strength [-]
$F$	Force [N]
$L$	Length [-]
$M$	Mach number [-]
$m$	Mass [kg]
$\dot{m}$	Mass flow [kg/s]
$M_w$	Molecular weight [g/mol]
$P$	Pressure [bar]
$p'$	Pressure pulsation [Pa]
$Pr$	Prandtl number [-]
$\dot{q}$	Energy rate [MJ/s]
$R$	Specific gas constant [J/kg K]
$\bar{R}$	Universal gas constant [J/mol K]

$Re$	Reynolds number [-]
$St$	Strouhal number [-]
$T$	Temperature [K]
$U$	Flow velocity [m/s]
$x$	Axial location in a pipe [m]
$z$	Compressibility factor [-]

### Greek symbols

$\alpha$	Acoustic attenuation [1/m]
	Impact angle [deg.]
$\gamma$	Specific heat ratio [-]
$\gamma^*$	Isentropic exponent [-]
$\Delta$	Differential [-]
$\partial$	Partial differential [-]
$\mu$	Dynamic Viscosity [kg/m s]
$\rho$	Density [kg/m <sup>3</sup> ]
$\Phi_P$	Dimensionless Power Spectral Density [Pa <sup>2</sup> /Hz]
$\phi_P$	Power Spectral Density [Pa <sup>2</sup> /Hz]

### Subscripts and superscripts

0	At rest
1	Gas "1" (hydrogen)
2	Gas "2" (natural gas)
a	absolute
g	gauge
l	internal
n	counter
p	particle
Sb	Side-branch
R	Material
r	ring
res	At resonance
th	thermowell
*	At choking.

## 1 Introduction

### 1.1 Relevance

The Netherlands has an extensive pipeline infrastructure for the transport and storage of natural gas. For reasons of personal and environmental safety and to ensure reliable supply, the infrastructure is built according to standards and norms for pipeline integrity. Currently, the reliability is ensured by complying with design codes [1] [2] [3] [4] and by using systematic approaches for maintenance and trouble-shooting [5] [6].

One of the main questions asked from a hydrogen transport point of view concerns the maximum allowable flow velocity under which risks related to asset and pipeline integrity are manageable and acceptable. As will be explained in more detail in chapter 2, energy transport capacity increases with higher pressures and higher flow velocities. To satisfy the selected transport conditions, compressors and pipelines are selected such that they render the lowest levelized cost of transport. As a rule though, a traditional limit of 20 m/s for the flow velocity is used in the natural gas transport industry (though deviations from this are also possible, for example some RNB operators use 30 m/s if the pressure is at least 3 bar(g)). This limit ensures that the appearance of integrity risks due to flow-induced vibration is minimized and remains at manageable levels further mitigated with engineering solutions. Occasionally, in the process piping of some assets, the flow speed can be larger. In large transmission pipelines, it normally is lower. Yet the limit of 20 m/s is referred to as a reasonable value to not be exceeded.

If hydrogen was to be transported considering the same limit as for natural gas, this would severely limit the capacity of existing pipelines to transport energy in the form of this carrier. Since hydrogen contains about 3 times less energy per unit volume, it would need to flow about 3 times faster to satisfy the same energy demand. Whereas it is not expected that hydrogen volumes will soon be such that this capacity is actually needed, it is important to understand what the risks are of transporting hydrogen at high speeds. Even if the same capacity as with natural gas was not required, allowing higher hydrogen flow velocities enables operating pipelines at lower pressure, which in turn leads to lower demands on compressor equipment and power required. In other words, can transport of hydrogen at nearly 3 times faster flow speed be achieved with a manageable impact on the network?

In HyDelta WP1E, the impact of high speed hydrogen flows is investigated. The survey includes the structural integrity of pipelines and pipeline equipment, but also other aspects such as noise radiation. Noise radiation is important for occupational safety as well as for comfort in the commercial and domestic environment. The objective is to establish a comparison between current service with natural gas and with hydrogen.

As a final introductory note: often, differences observed between hydrogen and natural gas are not directly linked to hydrogen as a fluid, but rather to the fact that it is assumed that the transport is done at high speed. Where informative, an explicit note will be made on whether the conclusions reached are connected to transport of hydrogen, the transport of a high speed gas, or both.

### 1.2 Scope of Work

The aim of this work package is to understand the impact of an increased flow velocity of H<sub>2</sub> on the different components of the existing gas transport and distribution infrastructure. In particular, the following impacts are in scope:

- Intrusive equipment such as thermowells
- Flow induced turbulence

- Flow induced pulsations
- Noise generation in piping and pressure reduction stations
- Erosion

As will be shown throughout the report, benchmarks between natural gas and hydrogen will be described for different aspects. Unless otherwise specified, only one natural gas composition has been used in this report: that is Groningen (G-) gas, as this is used throughout the Dutch gas transport and distribution system. In most cases, conclusions would hold when the comparison is done against high-calorific (H-) gas, though not always this is the case. In cases where the difference is slightly favourable or unfavourable to hydrogen, this may well be the opposite when comparing against H-gas. However this is only in cases where differences are small anyway.

The set of failure mechanisms connected to the compatibility of materials with hydrogen is widely studied in other (former and current) studies and explicitly excluded from the scope of this work package.

Finally, transport of hydrogen at lower velocities than those required for transporting the same amount of energy is not analysed in detail. This premise is currently considered conservative in some segments of the gas transport system, particularly the HTL system, and realistic for others such as the RNBs. Flows at lower speeds are of course also of interest, but for the subjects analysed in this report, lower flow speeds will in all cases show more benign results.

### 1.3 Earlier and parallel research

Process and transport systems operating with (nearly) pure hydrogen are covered by widely used engineering standards such as ASME B31.12 “Hydrogen Piping and Pipelines” [7]. Typically failure mechanisms covered in such document have to do with the material compatibility of the pipelines and components with hydrogen, for example hydrogen induced crack or hydrogen embrittlement. In addition to this, several projects are currently investigating the compatibility of existing gas transport systems and equipment to hydrogen or blends of natural gas and hydrogen. The North Sea Energy Program [8] or the HIGGS project [9] are examples thereof.

On the topic of maximum flow velocity for hydrogen, two references have been recently published while HyDelta was running. The first is from the H21 initiative [10], where it is stated that the current design limit for natural gas service is 40 m/s, due to erosion concerns. This is further limited to 20 m/s for “known dusty natural gas pipelines”. This report indicates that more research is ongoing to better understand how this will change with hydrogen service, but that hydrogen may be able to pick up less particles due to its lower density and viscosity. Steiner [11] in Germany correctly points to concerns about pressure drop, erosion, noise emission and vibrations and discusses why the current rule of thumb of 20 m/s is used with natural gas service. The author also formulates questions contained in this HyDelta WP as to what to expect once the flow speed has to be increased to maintain the energy rates with pure hydrogen, but no specific answers are offered. In the Netherlands, the limit of 20 m/s has been traditionally linked to pulsations and vibrations. No evidence of erosion being an issue is reported by GTS or RNB operators. This is due to the preventive measures put in place, but nonetheless the limits connected to erosion are relevant due to incidental or residual presence of solids inside the pipelines.

## 1.4 Gas Transport System

To better understand the conditions and parameters relevant to the benchmark, first an inventory of typical hardware present in the system is made. At the end of this section, the different subjects of this research are connected to the different segments of the gas transport and distribution system.

The Dutch gas transport system receives its gas from different sources and is roughly divided in four segments based on their pressure: the *Hoofd Transport Leidingstelsel* (HTL) and the *Regionaal Transport Leidingstelsel* (RTL), which are managed by GTS; and the *Regionale Netbeheerders* (RNB) systems. This is illustrated in Figure 1-1. The HTL is separated from the RTL by *Meet & Regel stations* (M&Rs, measuring and control stations) the pressure is reduced to typically 40 bar(g). Further downstream the system, gas is delivered to the local distribution grids, where pressure is reduced to typically 8 bar(g) in *Gas Ontvangst Stations* (GOS, gas-receiving station). Downstream the GOSs, the gas is further distributed by local gas net operators (RNBs). This is done via a grid of district stations, which reduce the pressure from typically 8 bar(g) to 30/100 mbar (g). The ultimate gas delivery may be done to small consumers (households) or larger industrial consumers. In the low-pressure grid, also parts may be operated at 4 bar(g) or 1 bar(g). In such cases, the pressure is reduced from 8 bar(g) in gas transfer stations (overslag stations). Further details on the design principles of the gas infrastructure can be found in [1] and [5].

Many assets located at the nodes and interfaces of these systems contain hardware that may be subject to high flow velocities, in particular:

- HTL system
  - o Transmission pipelines
  - o Compressor stations
  - o Storage Stations
  - o M & R stations
- RTL system
  - o Transmission pipelines
  - o GOS stations
- RNB systems
  - o Piping systems (HP, LP)
  - o Gas transfer stations
  - o District stations

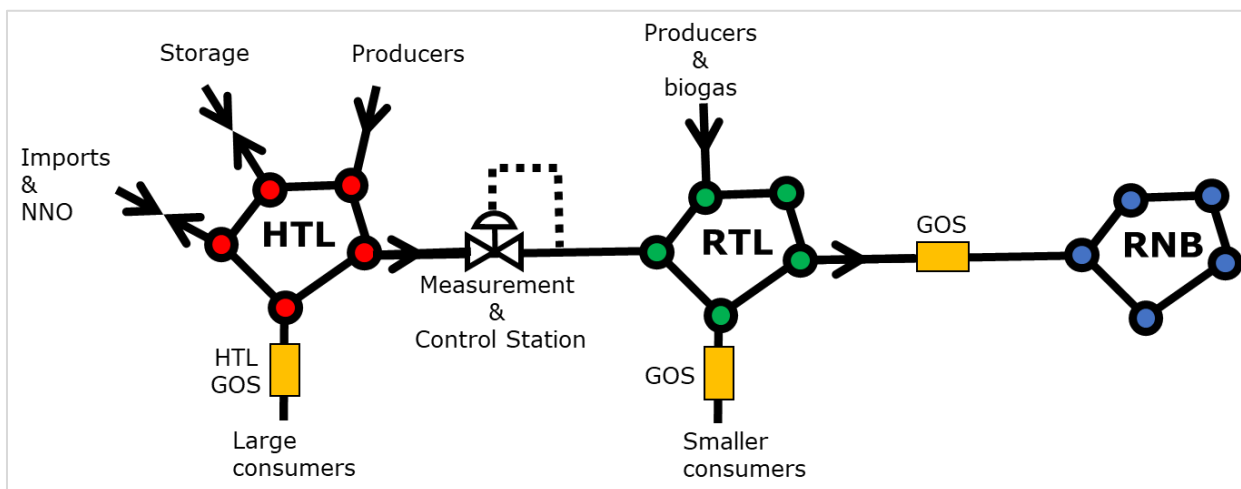


Figure 1-1 Overview of the Dutch gas transport and distribution system.

The type of hardware normally found in contact with the process fluid are as follows:

- Pipelines (of different materials).
- Fittings such as flanges, weldolets, reducers, etc.
- Restriction orifices.
- Scrubbers (filter, cyclone).
- Valves (all types, including safety relief valves).
- Compressors (centrifugal and reciprocating).
- Pulsation reduction elements (dampers, silencers).
- Coolers (and heaters e.g. at storage sites).
- Instrumentation such as flow meters, pressure gauges and thermometers/thermowells.
- Drying equipment.

In this work-package, fittings are excluded as their relevance is more connected to material compatibility and leak tightness, where flow itself does not play a relevant role. Impact of flow on scrubbers/filters is assessed in WP1B. Valves are investigated in other studies from the perspective of material compatibility, but this WP does cover the potential of valves for noise and turbulence generation (particularly control valves inducing large pressure drops). Compression equipment is excluded as hydrogen compression and mitigation strategies for resulting pulsations such as damper design is considered a mature technology [12]. The impact of flow velocity on flow metering is part of the investigations performed in WP1D, and thus it is also not included.

Table 1-1 shows the connection between the flow-related phenomena subject of this research (as listed in section 1.2) to the different segments of the Dutch gas transport and distribution system. Pressure drop is an important subject in all segments due to its connection to pipeline capacity, but less important in assets whose pressure loss is dominated by a pressure let down device such as a M&R station of a gas district station. Fatigue failure of intrusive equipment is typically only relevant at nodal locations of the network where measurements are taken, but not for the pipelines themselves. The same applies to flow-induced turbulence and acoustics induced vibration. Flow-induced pulsations are only relevant in the HTL and RTL part of the system (i.e. GTS and not RNBs). Flow-induced noise is also relevant only for nodes of the network due to occupational health and safety, but not for the transport pipelines. Due to the proximity to consumers, it is of interest to understand flow-induced noise for pipelines in the RNB systems. Erosion is a topic that applies anywhere with potential presence of solid particles. Due to several reasons, more importantly the preventive measures in place, this is not currently an issue with natural gas. However its effects would be important in all segments of the network and therefore the analysis scopes the typical conditions for all segments.

Table 1-1. Fundamental aspects related to flows at high-speeds and connection to the different segments of the gas transport and distribution system. For clarification please refer to accompanying notes in the main body of the text.

Segment of Gas System	Pressure drop	FIV Intrusive Equipment	Flow Induced Turbulence	Flow Induced Pulsations	Acoustics Induced Vibration	Flow Induced Noise	Erosion
HTL pipeline	x						x
HTL compressor station	x	x	x	x	x	x	x
HTL storage station	x	x	x	x	x	x	x
HTL M&R station	x	x	x	x	x	x	x
HTL GOS	x	x	x	x	x	x	x
RTL pipelines	x						x
RTL GOS	x	x	x	x	x	x	x
RNB pipelines HP	x	x				x	x
RNB pipelines LP	x	x				x	x
RNB gas transfer stations	x	x	x		x	x	x
RNB gas district stations	x	x	x		x	x	x
RNB up to household meter	x		x			x	x

## 1.5 Description of the report

In the first chapter after this introduction, chapter 2, the basic information concerning hydrogen transport and how it compares to natural gas (G-gas) is presented. After that, each chapter corresponds to each one of the questions introduced in the Scope of Work. Chapter 3 is devoted to the impact of hydrogen high speed flows on intrusive equipment, particularly (sheathed) thermometers and thermowells. The subject of flow-induced turbulence is introduced in chapter 4. Flow induced pulsations for hydrogen service are explored in chapter 5. Flow-induced noise and its potential consequences for integrity are described in chapter 6, whereas the radiation of such noise is covered in chapter 7. Finally, erosion is covered in chapter 8.

The structure of chapters 3-8 is always the same. Since the investigated subjects are also relevant to current network operation with natural gas, in general the first section is devoted to describing the existing situation with regards to that topic. For example: how are flow-induced pulsations dealt with nowadays, or what issues they can create. This is followed by a section describing how quantification of such risks is currently done. This is followed by a generic benchmark between natural gas and hydrogen based on the quantification methods described in the previous section. From the benchmark, general conclusions are offered. Application examples for typical hardware or configurations encountered in the Dutch gas transport system are offered to close each chapter.

A final overall summary and closing remarks are offered in chapter 9.

## 2 Hydrogen Transport

### 2.1 Energy Transport Capacity

Energy can be chemically stored in hydrogen (H<sub>2</sub>). As an energy carrier, hydrogen features a very high specific energy (i.e. per unit mass), whereas it features a very low energy density (i.e. per unit volume). Hydrogen is shown in comparison to other substances or technologies in Figure 2-1.

Volume and therefore pressure are very important parameters related to the transport and storage capacity of an eventual hydrogen-based energy system. These also define the eventual cost of the hardware that makes the energy infrastructure. Neglecting a number of second order effects: if the same amount of energy is to be transported with hydrogen and natural gas at similar pressures, hydrogen volumes must flow 3 times faster.

The equation for energy transport  $\dot{q}$  [MJ/s] depends on the mass flow  $\dot{m}$  [kg/s] and the energy content per unit mass of the substance expressed for instance by its higher heating value  $HHV$  [MJ/kg]. The lower heating value could also be used instead.

$$\dot{q} = \dot{m} HHV \quad (\text{eq. 1})$$

To make the effect of pressure explicit, at a particular reference location, this can be rewritten into:

$$\dot{q} = \frac{P}{z R T} U \frac{\pi (ID)^2}{4} HHV \quad (\text{eq. 2})$$

in which  $P$  is the absolute pressure [Pa(a)],  $z$  is the compressibility factor [-],  $R$  is the specific gas constant [J/kg K],  $T$  the absolute temperature [K],  $U$  is the flow velocity [m/s], and  $ID$  is the inner diameter of the pipe [m]. For pipeline transport, the physical design variables are then the pressure, the nominal pipe size with wall thickness and, finally, the flow velocity. They are all interconnected. For example, higher pressures require thicker walls, but the selected pipe size could be smaller; larger pipe sizes though reduce the pressure drop, lowering the load on compressors and improving overall system efficiency. Eventually, the final selection for a pipeline is made on the basis of an optimization yielding the lowest levelized cost of transport, which must include the entire transport system and not only the pipeline itself.

For instance, the capacity of a pipeline to transport energy as a function of its diameter is shown in Figure 2-2. The larger the pipe size or the pressure, the more hydrogen can be transported. As an example: a 42 inch (DN1050) pipeline at 60 bar(a) can transport 12 GW(th, HHV) at flow velocities of 20 m/s. A 10 inch pipeline (DN250) at 8 bar(g) can transport about 90 MW(th, HHV) at the same flow velocity.

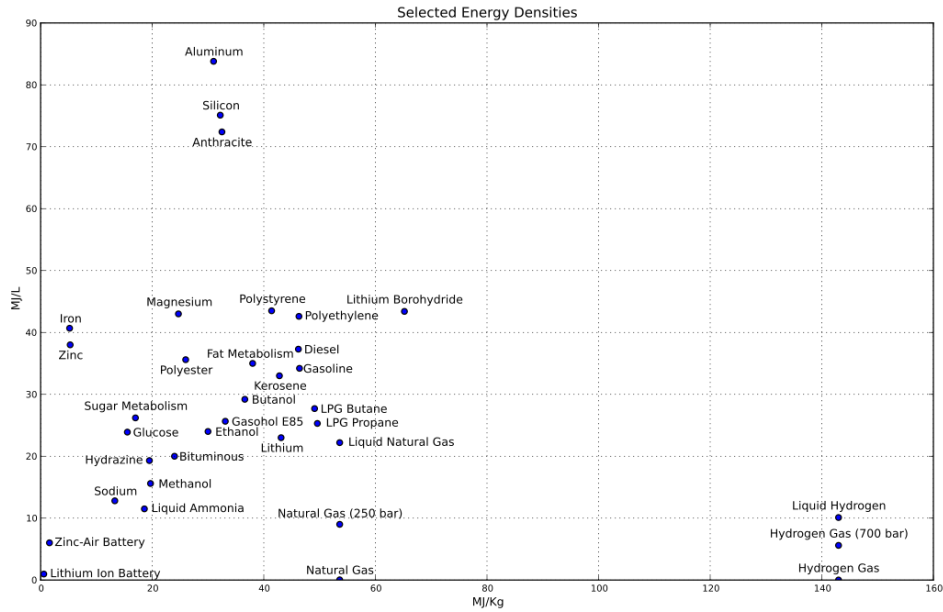


Figure 2-1. Energy density (x-axis) vs specific energy (y-axis) for a number of selected items. Hydrogen is found on the bottom right corner of this plot. Obtained from Ref. [13].

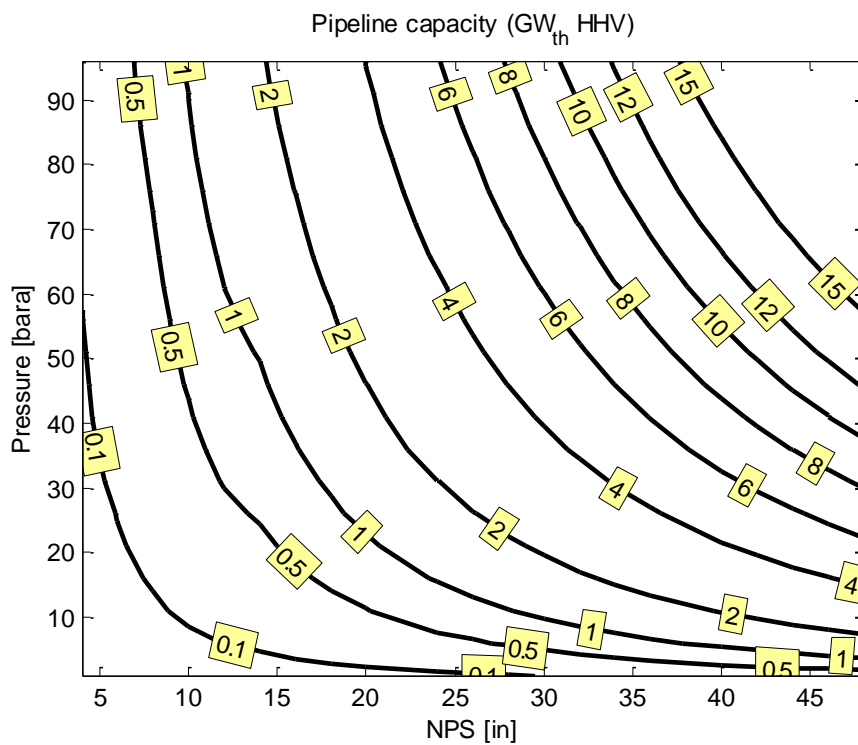


Figure 2-2. Energy transport capacity with  $H_2$  expressed in  $GW$  (thermal, HHV based) of different nominal pipe sizes (schedule XS) at different pressures. Reference conditions are assumed at a temperature of 10 deg. C and a flow velocity of 20 m/s.

## 2.2 Flow velocity ratio

In the previous, it has been discussed that the energy transport capacity of a pipeline is dependent on:

- Pipeline size
- Operating pressure
- Energy carrier (natural gas, hydrogen, blends thereof, etc)

The difference in flow velocity for two energy carriers to transport the same amount of energy can be obtained from (eq. 1), resulting in:

$$\frac{U_1}{U_2} = \frac{HHV_2}{HHV_1} \frac{\rho_2}{\rho_1} \quad (\text{eq. 3})$$

where  $\rho$  is the density of the fluid [kg/m<sup>3</sup>] at a given condition given by its pressure and temperature.

The flow velocity ratio needed to substitute G-gas by hydrogen and still transport the same amount of energy is given in Figure 2-3. Whereas the often quoted ratio of 3 is a good nominal rule of thumb, due to real-gas effects (the compressibility factor  $z$  given in (eq. 2)), this value can vary between ~ 3.4 for high pressure conditions and 2.7-2.8 for the RNB systems.

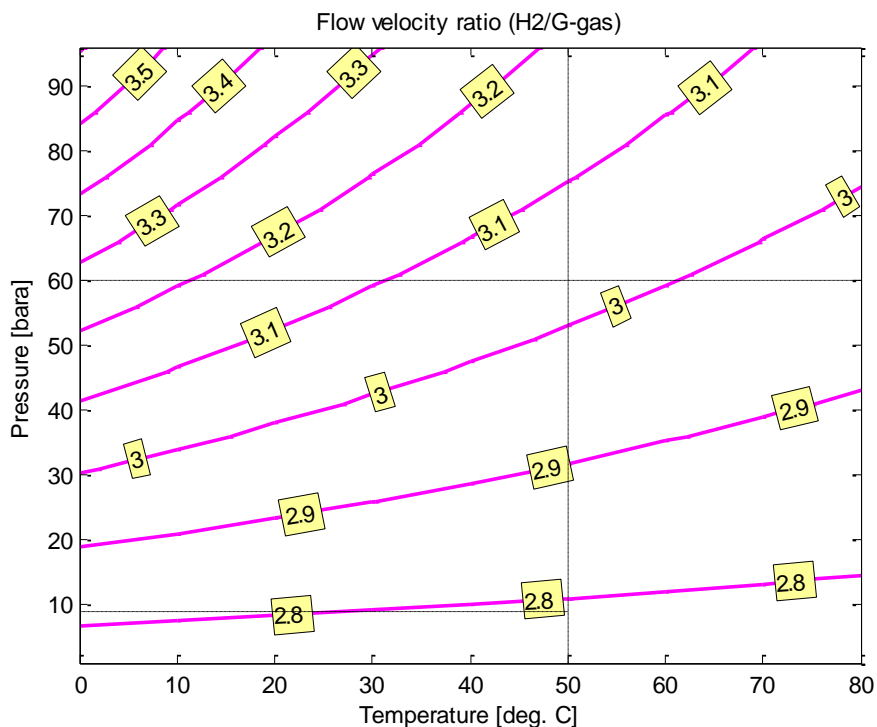


Figure 2-3. Flow velocity ratio between hydrogen and G-gas to obtain the same amount energy transport capacity (HHV-based). Dashed lines separate different regions of the energy transport system: high pressure and high temperature represent compressor discharge condition; high pressure and low temperature represent transport pipeline inlet conditions; intermediate pressures represent the regional transport system (RTL), and pressures below 8 bar(g) represent the RNB systems.

### 2.3 Pressure drop

The fluid flow through a pipeline is opposed by friction forces at the walls. The energy spent in overcoming this resistance results in pressure losses. The pressure gradient  $\partial P/\partial x$  at a particular axial location  $x$  of a (horizontal) pipeline is given by:

$$\frac{\partial P}{\partial x} = f \frac{1}{2} \rho U^2 \frac{1}{ID} \quad (\text{eq. 4})$$

In which  $f$  is the friction factor [-], which is a function of Reynolds number and sand grain roughness (a metric for the inner surface smoothness), i.e.  $f = f\left(Re, \frac{\epsilon}{ID}\right)$ . In the absence of heat transfer through the pipe walls, a reduction in fluid density is experienced which in turn makes the flow velocity increase, creating a larger pressure gradient. Therefore, the pressure losses are not constant throughout the length of the pipeline. Though exact solutions exist for different sets of assumptions, these eventually need to be solved numerically. Currently, the most convenient way to capture all physics involved is by means of one-dimensional hydraulic simulations.

In the simplest scenario of negligible pressure drop compared to the pipeline operating pressure, no heat transfer, and sufficiently high Reynolds number, (eq. 4) can be rewritten to yield the pressure losses  $\Delta P$  [Pa] from:

$$\Delta P = f \frac{1}{2} \rho U^2 \frac{\Delta x}{ID} \quad (\text{eq. 5})$$

In which  $f$  is the friction factor [-] and  $\Delta x$  is the pipeline length [m].

#### 2.3.1 Hydrogen vs G-gas

When (pure) hydrogen is compared to natural gas in terms of pressure drop only, the following transport parameters can be fixed to establish the comparison:

- Similar pressure and temperature ( $P, T$ )
- Similar pipe and surface quality/condition ( $ID, \epsilon$ )
- Same energy transport rate ( $\dot{q}$ )

In this scenario, the pressure drop difference between hydrogen and natural gas (G-gas) depends on the difference in Reynolds number and dynamic pressure ( $\frac{1}{2}\rho U^2$ ). Based on (eq. 3), for two fluids used to transport energy under the assumptions mentioned above, the ratio of Reynolds number is given by:

$$\frac{Re_1}{Re_2} = \frac{\mu_2}{\mu_1} \frac{HHV_2}{HHV_1} \quad (\text{eq. 6})$$

with  $\mu$  the dynamic viscosity [kg/m s]. The ratio of dynamic pressure is given by:

$$\frac{\frac{1}{2} \rho_1 U_1^2}{\frac{1}{2} \rho_2 U_2^2} = \left(\frac{HHV_2}{HHV_1}\right)^2 \left(\frac{\rho_2}{\rho_1}\right) \quad (\text{eq. 7})$$

The results for both ratios are given in Figure 2-4 and Figure 2-5. It is observed that the Reynolds number attained in hydrogen flow is 40-50% that of G-gas under the conditions given above, whereas the dynamic pressure is roughly the same. This means that in the limit in which the Reynolds number is high enough to not matter (constant friction factor), the pressure drop experienced in each scenario is approximately the same. Whether this limits applies is more likely to occur in the HTL part of the gas transport system due to its higher pressure, see Figure 2-6. The range of Reynolds number for HTL typical conditions is high enough, such that the friction factor is not altered when service is switched to hydrogen (at flow speeds corresponding to transporting the same amount of energy). However, the same does not apply to the RNB system. Due to the Reynolds number ratio also shown in Figure 2-4, an actual increase in friction factor is expected. That would mean at these low Reynolds numbers, the pressure drop may increase. An exception to this would still be possible if the pipes contained dust and sand throughout the length of the system. In such case, the region in which the friction factor is dominated by the surface quality occurs at a lower Reynolds number. This exception is not expected.

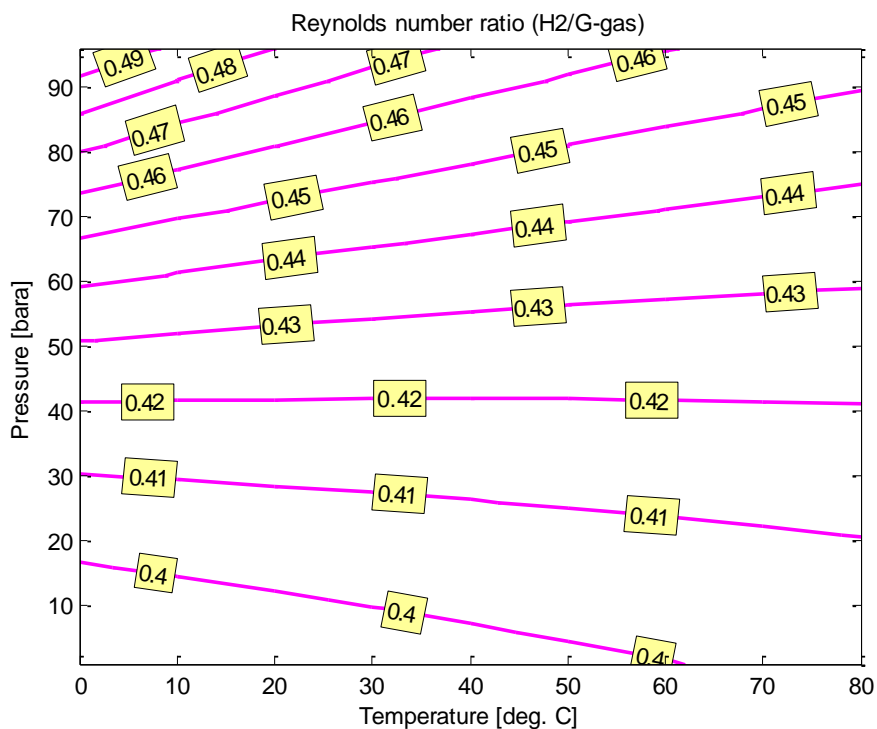


Figure 2-4. Reynolds number ratio between hydrogen and natural gas at equal operating conditions.

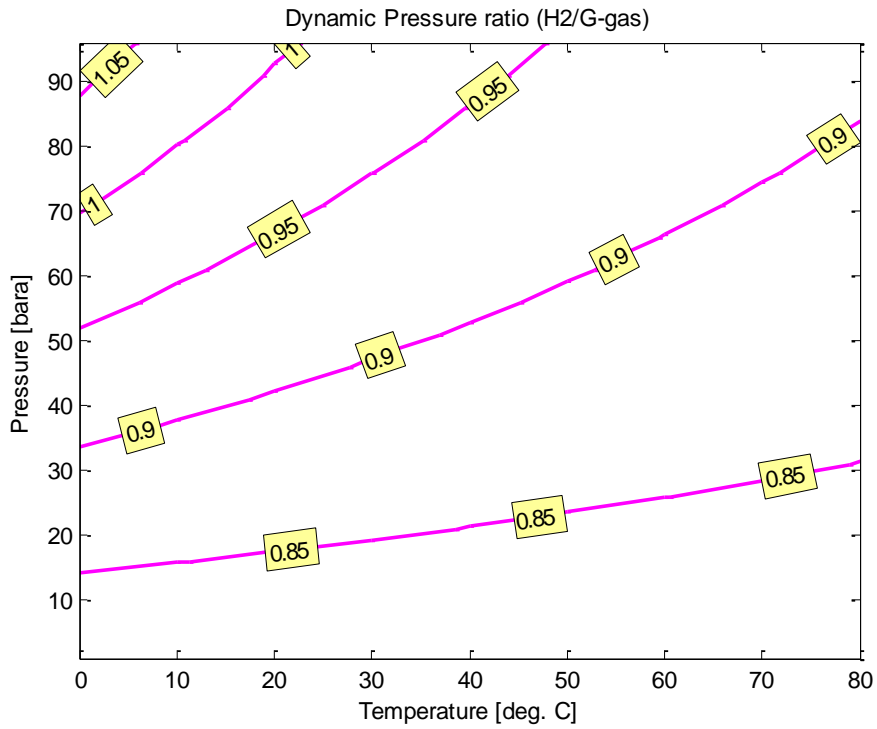


Figure 2-5. Dynamic pressure ratio between hydrogen and natural gas at equal operating conditions.

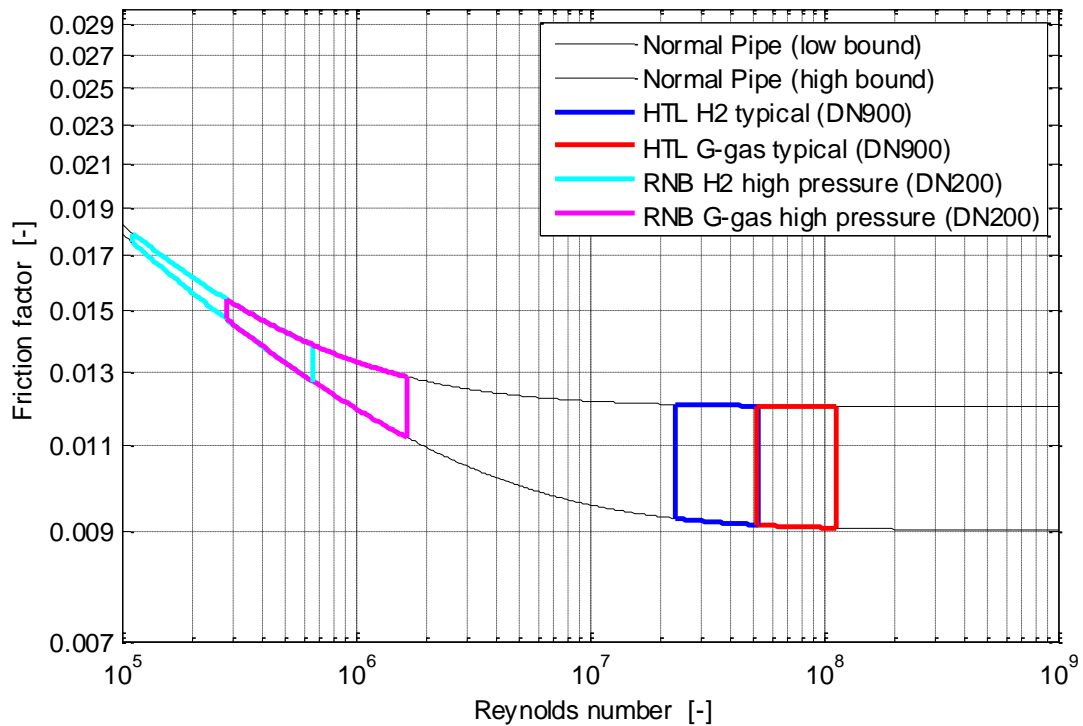


Figure 2-6. Friction factor as a function of Reynolds number for natural gas and hydrogen for HTL (> 40 bar(g), DN900) and RNB typical conditions (<8 bar(g), DN200).

### 2.3.1.1 Examples

To better understand the discussion presented above for practical situations, a number of examples is offered in Table 2-1. Examples correspond to a transmission pipeline of the HTL system, the HP segment of an RNB system and the LP segment of an RNB system close to domestic users. A fourth case for the configuration near domestic users is added to understand the effect of pipes with more solid contamination or materials with worse surface qualities. In these examples, the general picture is that the pressure losses are very similar when comparing natural gas and hydrogen at similar energy rates, as was expected from examination of Figure 2-5. In general, pressure drop is in favour of H<sub>2</sub> when the velocity ratio tends to be less than 3. In the case of clean pipes whose friction factor is not dominated by the surface quality (example 3), hydrogen has slightly larger losses. This is due to its reduced Reynolds number compared to G-gas, which increases the friction factor. This confirms earlier findings in references [8] [14].

From a pipeline capacity point of view and disregarding at this stage other potentially limiting factors (as discussed in further chapters of this report), the same energy rate can be transported with hydrogen as currently done with natural (G-)gas.

Table 2-1. Pressure drop gradients for different configurations with G-gas and hydrogen. The flow velocity for hydrogen is obtained from the values depicted in Figure 2-3.

Parameter	G-gas	H <sub>2</sub>						
Inner diameter [mm]	1200	1200	200	200	25	25	25	25
Surface roughness [μm]	50	50	20	20	20	20	100	100
Pressure [bar(g)]	80	80	8	8	0.1	0.1	0.1	0.1
Temperature [°C]	10	10	10	10	10	10	10	10
Flow velocity [m/s]	10	34	10	28	10	27.5	10	27.5
Density [kg/m <sup>3</sup> ]	75.0	6.6	7.2	0.768	0.793	0.0856	0.793	0.0856
Viscosity [kg/m s]	1.36E-05	8.70E-06	1.15E-05	8.60E-06	1.13E-05	8.60E-06	1.13E-05	8.60E-06
Reynolds # [-]	6.62E+07	3.10E+07	1.25E+06	5.00E+05	1.75E+04	6.84E+03	1.75E+04	6.84E+03
Darcy friction factor [-]	0.0103	0.0103	0.0131	0.0143	0.0280	0.0352	0.0333	0.0388
Pressure drop [bar/km]	0.321	0.329	0.236	0.215	0.444	0.456	0.528	0.503

### 3 Intrusive Equipment

#### 3.1 Intrusive equipment in natural gas transport systems

In process equipment and fluid transport systems, certain instrumentation needs to be in direct contact with the process medium, penetrating well into the bore of pipes. Examples of such instruments are for instance temperature gauges (thermowells), erosion probes as used in the upstream oil and gas industry, or V-cone flow meters. For gas transport systems, thermowells are the most common piece of equipment that penetrates into the flow. A potential risk for fatigue failure exists as a result of a coincidence between the natural frequency of the device and the vortex shedding frequency of the flow around the device. Vibrations in such condition can create large cyclic stresses near the root of the thermowell. When a thermowell fails, it can eventually be dislodged from its root and travel downstream in the pipe. The eventual damage that can unfold could thus be serious. The basic mechanism is analogous to large harmonic oscillations sometimes observed in road lighting masts in windy days.

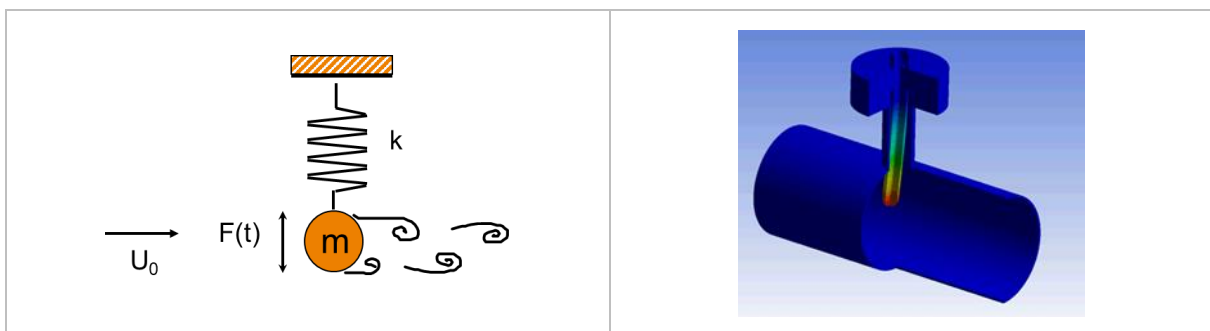


Figure 3-1. Left: fundamental mechanism for flow-induced vibrations; right: illustration of a thermowell undergoing harmonic oscillations (colour represents displacement from equilibrium position) as a result of a coincidence between vortex shedding around the stem of the device and its mechanical natural frequency.

#### 3.2 Assessment of flow-induced vibration for thermowells

The risk for this well-known failure mechanism can be assessed from two overlapping standards: the AVIFF guidelines [15] and ASME PTC 19.3 TW-2016 [16]. Some thermowell designs address the risk by incorporating vortex breakers, destroying the coherence of the vortex shedding mechanism and thus eliminating the risk. However, most existing devices in the gas grid today feature standard designs (straight, stepped or tapered).

In the basic approach to evaluate the risk for flow-induced vibrations, the fluid vortex shedding frequency around the thermowell and its mechanical natural frequency are calculated. The thermowell is considered a flexible beam. Aerodynamic forces act transversally to the axis of the thermowell: a fluctuating drag force is parallel to the flow, whereas a fluctuating lift force is perpendicular to the flow. Drag forces are exerted with the twice the frequency of lift forces, but they can be an order of magnitude weaker. A high risk is present when the vortex shedding frequency at the maximum possible flow velocity is higher than mechanical natural frequencies of the device, as that means that resonances can be excited during operation.

The reader can refer to the ASME PTC 19.3 TW-2016 [16] for a full description of the equations to be used. Here only the most important equation required to justify the benchmark between natural gas and hydrogen is explained. The vortex shedding frequency  $f_s$  [Hz] can be obtained from the dimensionless Strouhal number  $St_s$  [-] as follows:

$$St_s = \frac{f_s d_{th}}{U} \quad (\text{eq. 8})$$

in which  $d_{th}$  is the tip outer diameter of the thermowell [m], and  $U$  is the mean flow velocity in the main line [m/s]. For all high Reynolds number applications in excess of  $5 \times 10^5$ , the Strouhal number is 0.22.

In the benchmark between natural gas and hydrogen, only the fluid and its intended velocity are considered. It is assumed the thermowell design remains constant (re-use assumption) and thus all its mechanical properties (both natural gas and hydrogen have no added mass influence at gas transport conditions). Therefore, only (eq. 8) is necessary.

### 3.3 Benchmark between natural gas and hydrogen

For a given thermowell, the vortex shedding frequency  $f_s$  of hydrogen compared to that of natural gas is directly the flow velocity ratio, as already given by (eq. 3) and Figure 2-3. If the mechanical design of the thermowell is correctly sized to have mechanical natural frequencies well above the maximum possible vortex shedding frequency with natural gas, the margin needs to be in excess of  $\sim 3$  to still be compliant for hydrogen service (at similar energy transport rates).

### 3.4 Examples

Gasunie and Netbeheer Nederland have facilitated the HyDelta consortium with the dimensions of commonly encountered designs in the high-pressure Gas Transport System (GTS) as well as the distribution (RNB) networks:

- Short (100 mm) and a long (160 mm) protection sheet used for a thermometer suitable for service at maximum 80 bar(g), straight design. Labels A1 and A2.
- Short (90 mm) and long (140 mm) protection sheet used for a temperature sensor suitable for service at maximum 80 bar(g), tapered design. Labels B1 and B2.
- Short (95 mm) and long (120 mm) thermowells for service at maximum 20 bar(g), straight design. Labels C1 and C2.

The main dimensions of these thermowells as well as the results of the calculations are summarized in Table 3-1. The main observation is that short and tapered designs, as expected, show lower risk compared to long, straight designs. In these examples, A1, B1 and B2 could cope with hydrogen flow in all cases equivalent to natural gas service; possibly A2 and C1 could as well depending on the actual location; possibly C2 would need replacement unless it would be located at a point in the distribution network where flow velocities are moderate.

### 3.5 Conclusion

Because of the ambitious increase in flow velocity with hydrogen, the risk to encounter resonances is larger, because the vortex shedding frequency will increase proportionally. Whether the risk indeed exists has to be assessed in a case-by-case basis. In the examples analysed, replacement of thermowells is required at speeds above 28 m/s for RNBs and above 38 m/s for GTS.

Table 3-1. Summary of thermowell dimensions and resulting maximum allowable flow velocities following ref. [16].

Label	A1	A2	B1	B2	C1	C2
System	GTS	GTS	GTS	GTS	RNB	RNB
Shape	straight	straight	tapered	tapered	straight	straight
Nominal length [mm]	100	160	90	140	95	120
Design pressure [bar(g)]	80	80	80	80	20	20
TW Tip diameter [mm]	13	13	9.7	13	8	8
Strouhal number	0.22	0.22	0.22	0.22	0.22	0.22
First mechanical natural frequency [Hz]	5025	1644	3351	1907	3153	1971
Maximum allowable flow velocity [m/s]	118.8	38.9	91.4	69.4	45.9	28.7

## 4 Flow Induced Turbulence

### 4.1 Flow Induced Turbulence in natural gas transport systems

The flow of natural gas is in most parts of the network turbulent by nature. When the velocity of a fluid flow increases, the amplitude of stochastic fluctuations associated to the turbulence will increase. Depending on the construction of the pipes in which the gas flows, these fluctuations may eventually lead to vibrations. Especially at locations in which the direction of the flow change, such as elbows and tee's, the turbulent structures will more frequently organize themselves in particular length scales and become more energetic, increasing the risk of flow induced vibration. It is usual to understand pressure drop as a metric of the turbulent fluctuations appearing in the flow: the larger the pressure drop, the more fluctuations arise.

Because flow-induced turbulence depends strongly on the kinetic energy of the flow, issues are more likely to occur in the high pressure system. For example, for G-gas at 0.1 bar(g) typical of the end of the distribution network, the flow would need to flow in excess of 75 m/s to even have a small chance to excite vibrations. At 60 bar(g), this number goes down to about 9 m/s, which is well within the realistic operation of high-pressure assets. In general, though, flow induced vibrations due to turbulence are not an issue in gas transport systems, as pipe supporting layouts are largely sufficient to arrest any motion that such flow fluctuations may cause.

### 4.2 Assessment of flow-induced turbulence

The Energy Institute Guidelines for Avoidance of Vibration Induced Fatigue Failure [15] provide the most common method to assess the risk of flow induced vibration. A score Likelihood of Failure LoF is defined to assess the risk due to flow-induced turbulence:

$$LoF = FVF \frac{\rho U^2}{F_V} \quad (\text{eq. 9})$$

where  $FVF$  is the fluid viscosity factor,  $\rho$  is the fluid density,  $U$  is the mean flow velocity and  $F_V$  is the flow induced vibration factor. The fluid viscosity factor depends only on the fluid viscosity. The flow induced vibration parameter depends only on the mechanical construction of the piping layout.

### 4.3 Benchmark between natural gas and hydrogen

Assuming that the mechanical construction of pipes will either be the exact same or similar in the case of hydrogen service, and introducing the definition of the  $FVF$ , the  $LoF$  ratio of two fluids scales as follows:

$$\frac{LoF_1}{LoF_2} = \sqrt{\frac{\mu_1 \rho_1 U_1^2}{\mu_2 \rho_2 U_2^2}} \quad (\text{eq. 10})$$

When hydrogen and natural gas (G-gas) are compared at equal energy rates and operational conditions, the results shown in Figure 4-1 are obtained. It is observed that for all conditions experienced in the Dutch natural gas transmission system, the risk for flow induced vibration due to turbulence is lower in hydrogen service than with G-gas service.

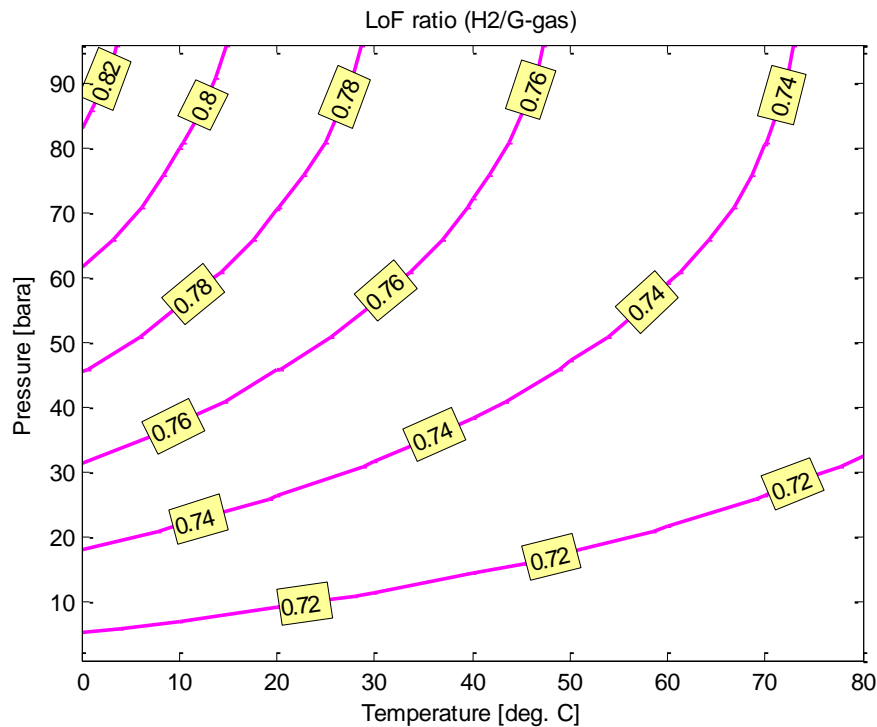


Figure 4-1. Ratio of LoF score obtained when hydrogen is compared to natural gas at similar energy transport capacities and operating conditions.

#### 4.4 Examples

Two examples are given in Table 4-1 to illustrate the conclusions obtained in this chapter. It is observed that the LoF scores are well below the first threshold level demanding any further attention (LoF > 0.3).

#### 4.5 Conclusion

The risk for flow-induced turbulence in hydrogen service is lower even at significantly higher flow velocities necessary to transport the same amount of energy. Since this mechanism is typically not an issue in natural gas transport systems, it will remain so in hydrogen transport systems.

Table 4-1. Examples of flow induced vibration risk calculation for the gas transport system, assuming medium-stiff pipe layout and typical pipe wall thicknesses.

	GTS		RNB	
	G-Gas	H <sub>2</sub>	G-gas	H <sub>2</sub>
<b>Pressure [bara]</b>	60	60	1.1	1.1
<b>Flow velocity [m/s]</b>	20	64	20	55
<b>Pipe diameter (DN)</b>	900	900	100	100
<b>FVF [-]</b>	0.113	0.093	0.107	0.093
<b>Kinetic Energy [kg/ m s<sup>2</sup>]</b>	21800	20480	316	259
<b>LoF [-]</b>	0.097	0.075	0.004	0.003

## 5 Flow Induced Pulsations

### 5.1 Flow induced pulsations in natural gas transport systems

Flow-induced pulsations (FIP) can arise as a result of a flow-acoustic interaction, typically when flow passes by dead-leg side-branches. The interaction occurs if the frequency of the acoustic source (shear layer instability) is similar to acoustic resonance frequencies of the piping. Severe vibrations can develop if also mechanical natural frequencies of the pipe assembly coincide with this frequency. Sustained operation with such vibrations can lead to fatigue failure. Besides mechanical failures, noise and flow metering errors can also be caused by high pulsation levels. Integrity risks due to flow induced pulsations are only relevant in the assets of GTS, because high pressures are needed to generate energetic enough forces to create damage. RNB systems are thus not affected by FIP risks.

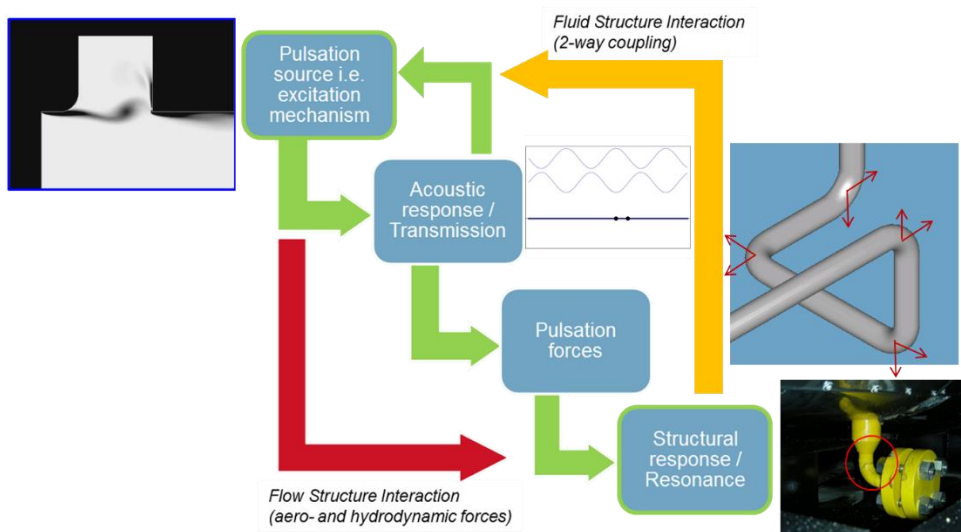


Figure 5-1 An interaction between flow instabilities and acoustic resonance can develop mechanical vibrations and eventually fatigue failure.

### 5.2 Assessment of flow-induced pulsations

For a given piping geometry, the source frequency depends on the flow velocity, whereas the acoustic resonance frequencies depends on the speed of sound of the medium. Therefore, for a given dead-leg geometry characterized by its length  $L_{sb}$  and its inner diameter  $d_{sb}$ , resonant conditions occur in the vicinity of particular Mach numbers that can be denoted resonance Mach numbers  $M_{res}$  (ratio between actual flow velocity and speed of sound). The different resonant acoustic modes  $n$  of a dead-leg side branch configuration then occur at:

$$M_n^{res} = \left( \frac{2n - 1}{4} \right) \left( \frac{d_{sb}}{L_{sb}} \right) \left( \frac{1}{Sr} \right) \quad (\text{eq. 11})$$

where  $Sr$  is the Strouhal number of the vortex shedding mechanism at T-joints, defined as:

$$Sr = \frac{f d_{SB}}{U} \quad (\text{eq. 12})$$

in which  $f$  is the central frequency of the vortex shedding [Hz],  $U$  is the mean flow velocity in the main line [m/s]. This equation is the same as (eq. 8) but using a different characteristic length.

Once a resonance condition has been established, the eventual pulsation amplitude  $p'$  is determined by an energy balance between the amount of flow kinetic energy converted into acoustic energy, and the dissipation of acoustic energy due to visco-thermal attenuation and radiation to the rest of the pipe system. The conversion efficiency of the aeroacoustic source is denoted  $F$ , and the acoustic attenuation  $\alpha_0$  [1/m]. In that case, the eventual pulsation amplitude  $p'$  [Pa] is:

$$p' = \rho U^2 \left( \frac{2 F}{\alpha_0 L_{sb}} \right) \quad (\text{eq. 13})$$

with  $\rho$  the fluid density of the medium [kg/m<sup>3</sup>].

In order to be able to predict flow-induced pulsations, it is essential to make appropriate choices for the Strouhal number and the source strength, which are known to depend on many parameters, such as Reynolds number, flow path-acoustic path configuration, edge rounding, distance to elbows and even non-linear effects such as eventual pulsation amplitude (saturation).

### 5.3 Benchmark between natural gas and hydrogen

When benchmarking natural gas and hydrogen it is assumed that the pipework design is the same, which is equivalent to a re-use scenario. In that case, the comparison between natural gas and hydrogen concerns primarily two questions:

- Which acoustic resonances can develop with hydrogen?
- What pulsation levels can be expected?

#### 5.3.1 Pulsation resonances

As explained in the previous section, resonances develop around particular Mach numbers. The ratio of Mach numbers between hydrogen and natural gas at equal operating conditions and energy transport rates is given by:

$$\frac{M_1}{M_2} = \left( \frac{U_1}{U_2} \right) \left( \frac{c_2}{c_1} \right) \quad (\text{eq. 14})$$

With  $c$  the speed of sound [m/s]. The flow velocity ratio has been shown in Figure 2-3 (eq. 3). The ratio of speed of sound is given in Figure 5-2. Since the ratios are very similar, their effect fundamentally cancels out: resonances are expected at similar energy rates.

Under equal energy rate and operating conditions, the Mach number for H<sub>2</sub> service tends to be slightly lower than for G-gas (see Figure 5-3). Since the Mach numbers associated to resonance are independent of the fluid, resonance conditions with H<sub>2</sub> will be reached at slightly higher velocities than those of G-gas. A similar interpretation is that resonance can be found at somewhat longer dead-legs when the same energy rate is transported.

Despite the similarities, an important difference between hydrogen and natural gas is the absolute frequency at which pulsations will develop, which will be approximately 3 times higher for hydrogen. For the same pipe geometry, resonances that could occur with natural gas at e.g. ~10 Hz, would develop at ~ 30 Hz with hydrogen, increasing the chance of coincidence with mechanical natural frequencies.

Concluding: hydrogen duty is associated to a similar risk of FIP resonance, and the differences are well within the typical uncertainties associated to the assumptions taken and the lock-in range of flow-induced pulsations. Due to the shift in frequency, the chance for coincidence with mechanical natural frequencies of the piping is increased.

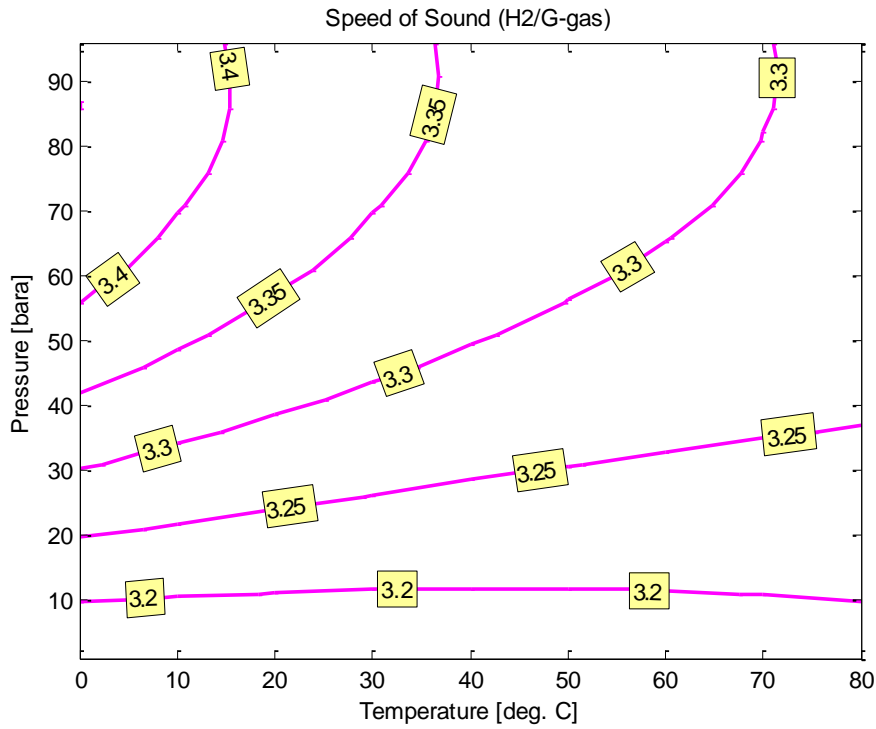


Figure 5-2. Ratio of speed of sound of hydrogen vs G-gas at equal pressure and temperature.

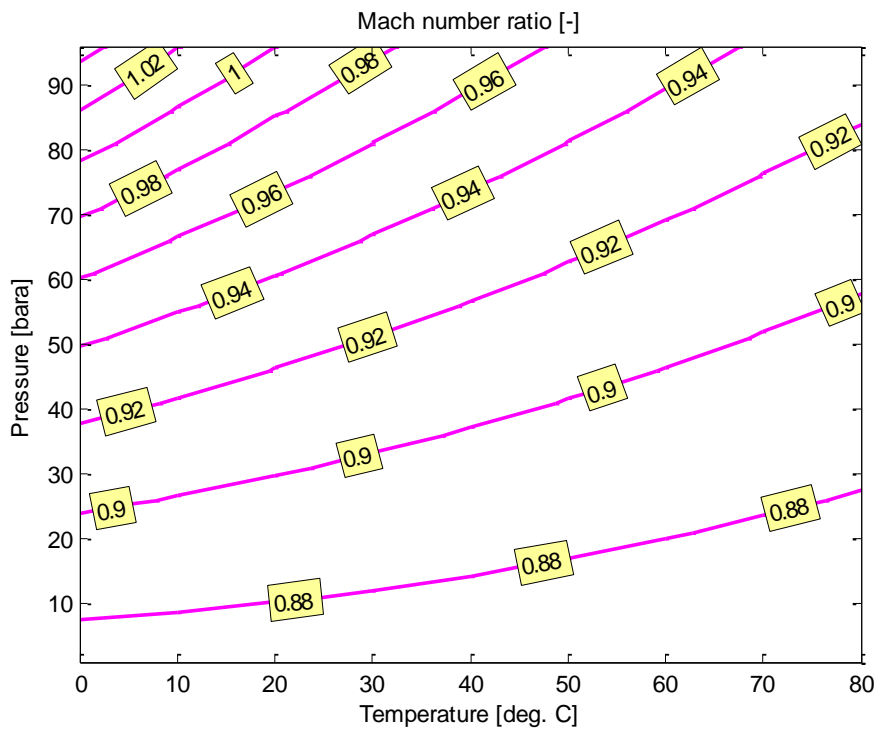


Figure 5-3. Ratio of Mach number of hydrogen and G-gas at equal energy transport rate.

### 5.3.2 Pulsation amplitudes

The flow-induced pulsation levels expected at resonances hit with hydrogen compared to those hit with natural gas can be inferred from (eq. 13). The ratio between the levels is then found from:

$$\frac{p'_1}{p'_2} = \frac{(\rho U^2)_1}{(\rho U^2)_2} \left(\frac{F_1}{F_2}\right) \left(\frac{\alpha_{0,2}}{\alpha_{0,1}}\right) \quad (\text{eq. 15})$$

For the first term of (eq. 15), i.e. the ratio of kinetic energy or dynamic pressure (eq. 7) can be used. For the second term, when assuming that the piping configuration is the same and the Reynolds number is high enough, then the dimensionless source strength  $F$  is the same for hydrogen and G-gas. Finally, the acoustic attenuation term can be found following:

$$\frac{\alpha_{0,1}}{\alpha_{0,2}} = \left(\frac{K_1}{K_2}\right) \left(\frac{M_1}{M_2}\right) \left(\frac{Re_2}{Re_1}\right)^{\frac{1}{2}} \quad (\text{eq. 16})$$

Where  $K$  is a factor connected to viscothermal acoustic losses:

$$K = 1 + \frac{\gamma^* - 1}{\sqrt{Pr}} \quad (\text{eq. 17})$$

with  $Pr$  the Prandtl number and  $\gamma^*$  the isentropic exponent of the fluid.

The acoustic attenuation ratio between hydrogen and natural gas is shown in Figure 5-4. More acoustic attenuation is expected in the case of hydrogen. The benefit of larger attenuation values with hydrogen is also observed in the ratio of eventual pulsation levels, shown in Figure 5-5. Pulsation levels about 40% lower can be expected compared to natural gas when a resonance develops.

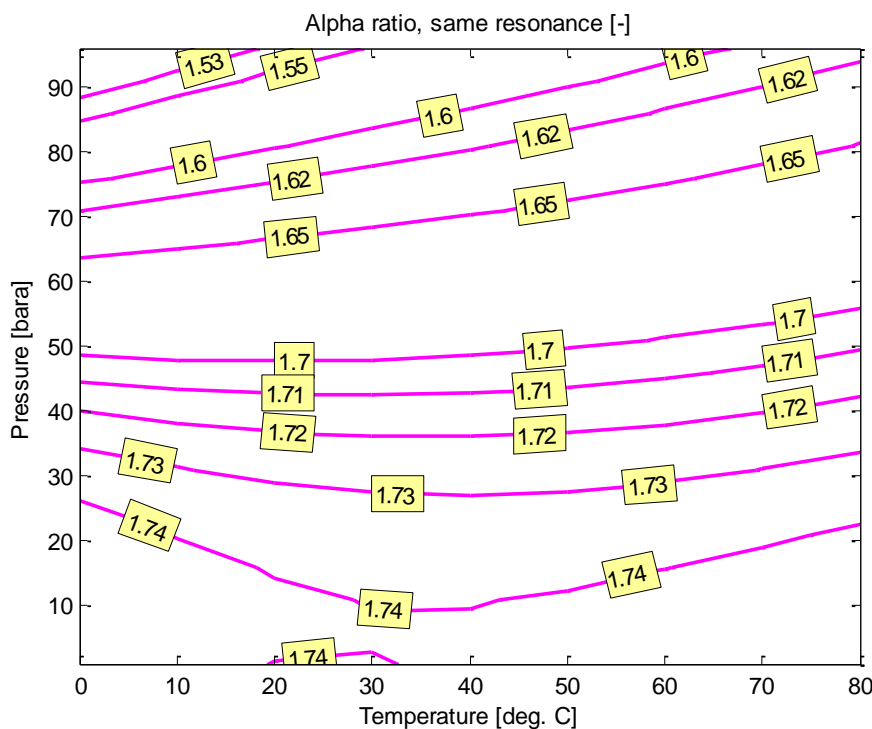


Figure 5-4. Ratio of acoustic attenuation between hydrogen and G-gas.

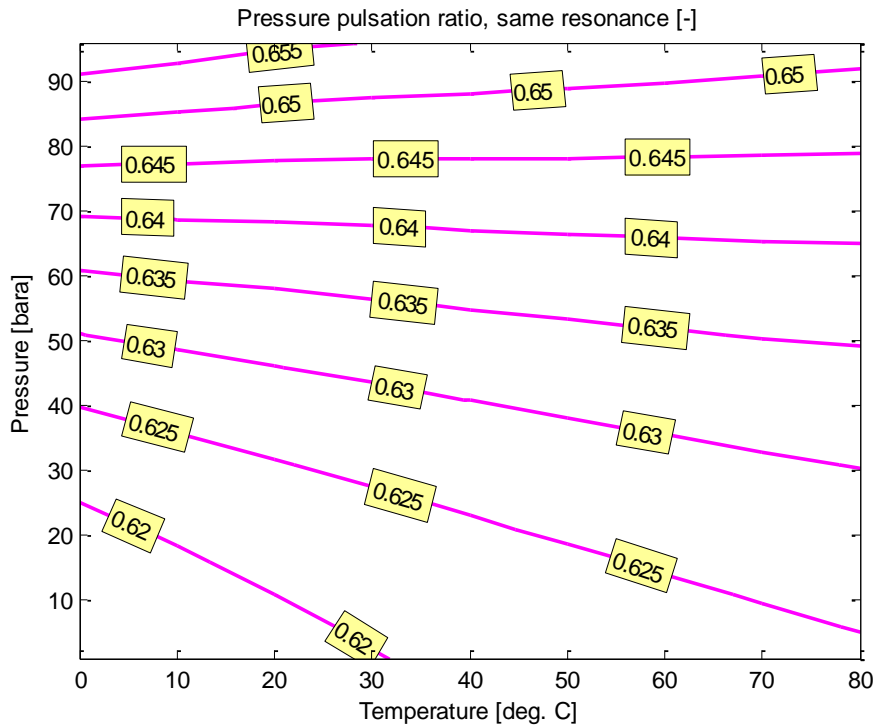


Figure 5-5. Ratio of pulsation levels between hydrogen and G-gas.

## 5.4 Examples

### 5.4.1 Case with natural gas

An example applied to a flow regulating station that suffered from severe flow-induced pulsations is offered for illustration. The geometry of the manifold is shown in Figure 5-6. The natural gas flow entered the pressure reduction street from the 20" inflow header at 60 bar(g). The flow speed in the 6" street was increased as a result of the 6"x4" reducers leading to the pressure regulator. Two twin 2" dead-legs meant for venting are tied into the 4" segment. The gas velocity in the 4" segment varied between no flow in case the regulator valve was closed, and 56.6 m/s, the maximum allowable flow through the regulator valve.

### 5.4.2 Case with hydrogen

If it is assumed that hydrogen may flow through the same flow regulating station, the comparison metrics shown in Table 5-1 are to be expected. In this example, it is observed that the same resonance observed with G-gas would be observed with hydrogen, but at slightly larger energy transport capacities. In such a case, the expected pulsation level would be significantly lower. However, the resonance would feature a much higher frequency (666 Hz) resulting in a larger chance of coincidence with a mechanical resonance. In such case, the general conclusion is that the perceived risk due to vibrations is larger. However, at such high frequencies, the eventual vibration amplitudes are to a large extent dominated by the mechanical damping of the assembly, which is extremely dependent on the design and condition of the assembly itself.

## 5.5 Conclusion

When comparing hydrogen with G-gas transporting the same energy rate through the same pipe assemblies at the same operating conditions, the following is concluded:

- Acoustic resonances will develop at similar energy rates

- Acoustic resonances will develop at  $\sim 3$  times higher frequencies, increasing the chance to coincide with mechanical natural frequencies
- Resulting pulsation levels will be lower with hydrogen, approximately 40%.

Two opposing effects arise: on the one hand the expectation of lower pulsation levels; on the other, a higher risk of coincidence between acoustic pulsations and mechanical natural frequencies. The net outcome of those effects can only be judged on a case-by-case basis, as high frequency vibrations largely depend on the mechanical damping of the assembly. To better understand whether the risk *tends* to increase or to decrease *in general*, 3D finite element analysis of a number of typical assemblies is recommended, whereby the modelled pipework is excited by high frequency pulsations and the cyclic stress levels are computed at critical spots more prone to failure due to stress intensification.

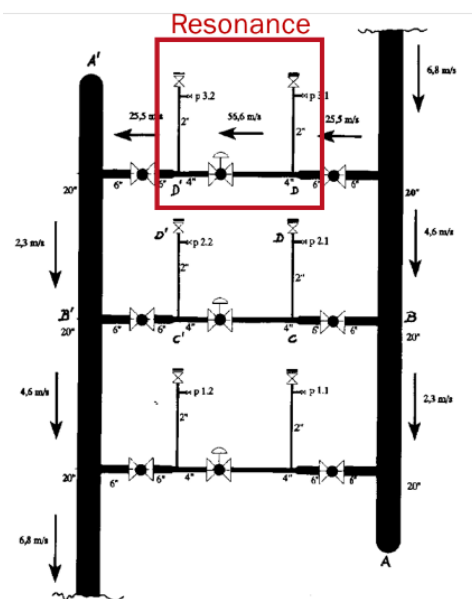


Figure 5-6. Schematic of a pressure reduction manifold with a double small side-branch configuration that showed severe flow-induced pulsations.

Table 5-1. Comparison between G-gas and hydrogen for a flow-induced pulsation.

Property	G-gas	Hydrogen	Notes
Pressure [bar(g)]	60	60	Operation assumed at same pressure
Temperature [°C]	10	10	Operation assumed at same temperature
Gas density [kg/m <sup>3</sup> ]	54.5	5.0	Compressibility factor z for G-gas $\sim 0.88$
Speed of sound [m/s]	395	1335	See Figure 5-2
Flow velocity at resonance [m/s]	41.0	138.6	Calculated from resonance Mach number
Mach number at resonance [-]	0.10	0.10	Resonances occur at same resonance Mach numbers
Resonance frequency [Hz]	197	666	
Pulsation levels [mbar rms]	1200	763	See Figure 5-5.
Energy rate at resonance	47.8	49.9	Hydrogen slightly larger energy transport capacity for same resonant conditions

## 6 Acoustics Induced Vibration

### 6.1 Acoustics-Induced Vibration in natural gas transport systems

Acoustics-Induced Vibration (AIV) concerns the failure mechanism by which a high-frequency broadband spectrum of noise rapidly leads pipework to fatigue failure. Typical sources of AIV in natural gas transmission systems are elements in which pressure is suddenly reduced: relief or blow-down valves, control valves and restriction orifices. The generated acoustic spectrum has a typical broadband character ('roaring' at lower frequency range, 'screaming' at the higher frequency range). The noise is characterized by its amplitude and by the peak frequency, see Figure 6-1. Noise generated by pressure let-down devices may lead to integrity issues. Incidents have been reported in literature but are relatively rare. Areas at increased risk are:

- Configurations with high in-line noise levels.
- Lines with large pipe diameter and small wall thickness.
- Configurations with welded discontinuities, such as small branch connection to a parent pipe, T-joints and welded pipe shoes. Circumferential welding, for example at elbows and flanges is not considered a critical discontinuity

Besides fatigue failure, noise radiation (potentially even metering errors) is also a consequence of this phenomenon. This is discussed in chapter 7.

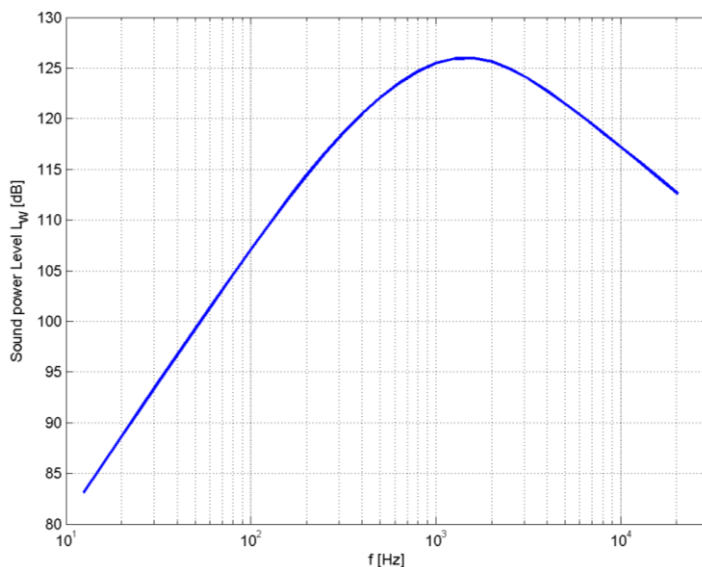


Figure 6-1. Typical frequency spectrum of noise due to pressure reduction devices: broadband spectrum with a broad peak around the centre frequency (~1.5 kHz in this example).

### 6.2 Assessment of Acoustics-Induced Vibration

Accurate quantitative prediction of amplitude and frequency of the acoustic source spectrum requires a very complex analysis. This is due to the physical phenomena occurring in case of pressure reduction (gas dynamics with choking flow conditions, complex fluid path, interaction with complex geometric structure of the valve cage, high-frequency 3D propagation of noise through pipe system and through pipe wall, details of the installation etc). Detailed prediction methods are still topic of academic research. To enable robust assessment of the risk and effective engineering, simplified industry standards have been developed in the past decades [15], [17], [18].

The first standard used to quantify the severity of pressure reduction devices is the Energy Institute “Guidelines for Avoidance of Vibration Induced Fatigue Failure” [15]. In these guidelines, the broadband noise caused by valves and orifices is referred to as “High-Frequency Acoustic Excitation”. The relevant section is technical module T2.7. The prediction models in [15] were developed based on empirical work conducted in the 70s, for failing and non-failing systems. Therefore it provides a metric for the risk of failure, and it should not be interpreted as an actual, numerical prediction of the expected noise levels inside the pipe. However, the correct scaling parameters are included. The power level of the source is quantified as:

$$PWL = 10 \log_{10} \left[ \left( \frac{P_0 - P_2}{P_0} \right)^{3.6} \dot{m}^2 \left( \frac{T_0}{M_W} \right)^{1.2} \right] + 126.1 + SFF \quad (\text{eq. 18})$$

The source power level  $PWL$  is a function of pressure differential  $(P_0 - P_2)/P_0$ , mass flow  $\dot{m}$ , inlet temperature  $T_0$  and molecular weight  $M_W$ . The factor  $SFF$  is a penalty of 6 dB in case of choking conditions. This equation indicates that the pressure differential and the mass flow are the dominant parameters; larger pressure differential and larger mass flow lead to increased noise levels.

### 6.3 Benchmark between natural gas and hydrogen

The basis of the benchmark is again that the same energy transport capacity is realised with hydrogen as with natural gas. This scaling approach is considered appropriate for continuous, in-line pressure reduction items (control valves in M&R stations, GOSs, district stations and transfer stations). For the incidental pressure reduction items (blow-down facility) the assumption of ‘equal energy flux’ is less obvious. However, assuming a re-use of blow-down valves and orifice plates, the same ratio (1:3) for the mass flows is expected.

To arrive at the incremental effect of hydrogen (subscript 1), compared to natural gas (subscript 2), the following relation is found for choking flow. This is obtained by assuming equal pressure ratios and the same valve internals, such that the difference is mostly due to critical (sonic) mass flow ratio:

$$PWL_1 - PWL_2 = 10 \log_{10} \left( \frac{\left( \frac{\rho_1}{\rho_2} \right) \left( \frac{2}{\gamma_1 + 1} \right)^{\frac{\gamma_1 + 1}{\gamma_1 - 1}} \left( \frac{M_{W,2}}{M_{W,1}} \right)^{1.2} \frac{\gamma_1}{\gamma_2}}{\left( \frac{2}{\gamma_2 + 1} \right)^{\frac{\gamma_2 + 1}{\gamma_2 - 1}}} \right) \quad (\text{eq. 19})$$

in which  $\rho$  is the density and  $\gamma$  the ratio of specific heats. If non-choking conditions exist, the following relation is found, which follows the mass flow ratio to keep the same energy transport rate, assuming again the same subcritical pressure jump :

$$PWL_1 - PWL_2 = 10 \log_{10} \left( \left( \frac{HHV_2}{HHV_1} \right)^2 \left( \frac{M_{W,2}}{M_{W,1}} \right)^{1.2} \right) \quad (\text{eq. 20})$$

Figure 6-2 illustrates these equations for various pressure and temperature conditions. The following observations are made, comparing hydrogen with natural gas:

- For non-choking conditions, an increase of 2-3 dB regardless of the operating conditions at which the benchmark is made.
- For choking conditions, a small increase 0-2 dB for high-pressure applications (40-80 bar)
- For choking conditions, an increase 2 dB for low-pressure applications (< 8 bar)

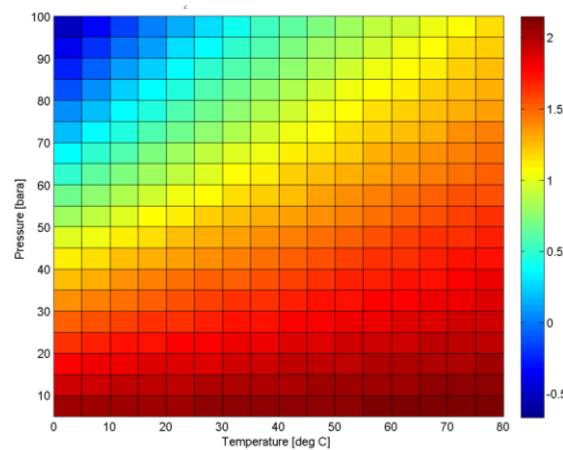


Figure 6-2. Comparison of noise source strength (choking condition).

### 6.4 Examples

In absolute terms, the most critical areas are the large-capacity blow-down configurations in the HP network. No reported examples to fatigue failures in the LP could be found in literature (for operation with natural gas). When an increased risk for failure is determined, a typical follow-up analysis considers coincidence between transversal acoustic resonances and structural shell modes of the pipes. This coincidence is illustrated in Figure 6-3 depicting modes with 11 nodal diameters, i.e. 11 wave characteristic lengths fit the perimeter of the pipe.

Two examples have been used for follow-up analysis of this coincidence. The first is a typical (steel) 36" (DN900) HP line of the GTS system; the second example is a typical (steel) 8" (DN200) of the HP segment of an RNB system. The analysis is based on a comparison between frequency and mode shape (represented by the number of nodal lines and nodal circles) of both the acoustic resonance mode and the structural shell mode. The results for each example are respectively shown in Figure 6-4 and Figure 6-5 . It is observed that, in both cases, the separation acoustical transversal resonance modes and the structural modes of the pipe wall increases with hydrogen compared to natural gas, which reduces the chance for detrimental coincidence. This is due to the higher speed of sound of hydrogen. Note that the acoustic modes shift to higher frequencies, due to the larger speed of sound in hydrogen. The pipe structural resonance modes are primarily a property of the pipe wall and will remain similar. In case of hydrogen, the chance that acoustic modes trigger pipe resonance modes and lead to integrity issues on the branch connections is reduced.

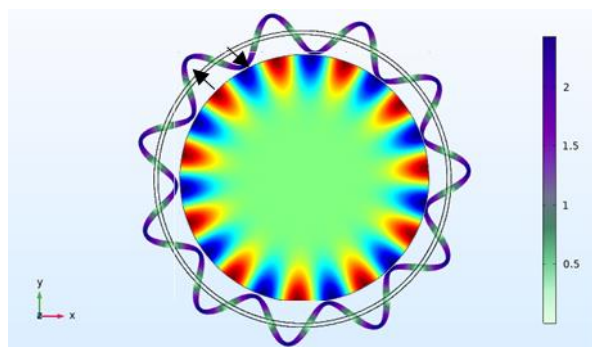


Figure 6-3 Example of coincidence between acoustic resonance mode and pipe resonance mode, featuring 11 nodal diameters. Acoustic energy can be very efficiently transferred into the vibration of the pipe wall.

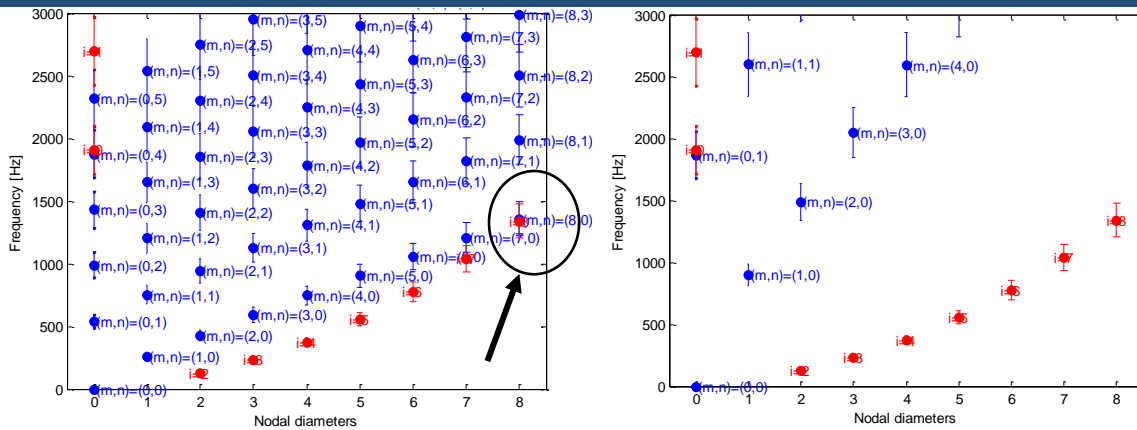


Figure 6-4. Typical interference diagram for HP system (36" line, 80 bara) displaying the frequency at which different resonance modes occur. Natural gas (left) and hydrogen (right). Blue dots are acoustic modes, red dots are structural modes. Coincidence risks is more prominent for natural gas than for hydrogen.

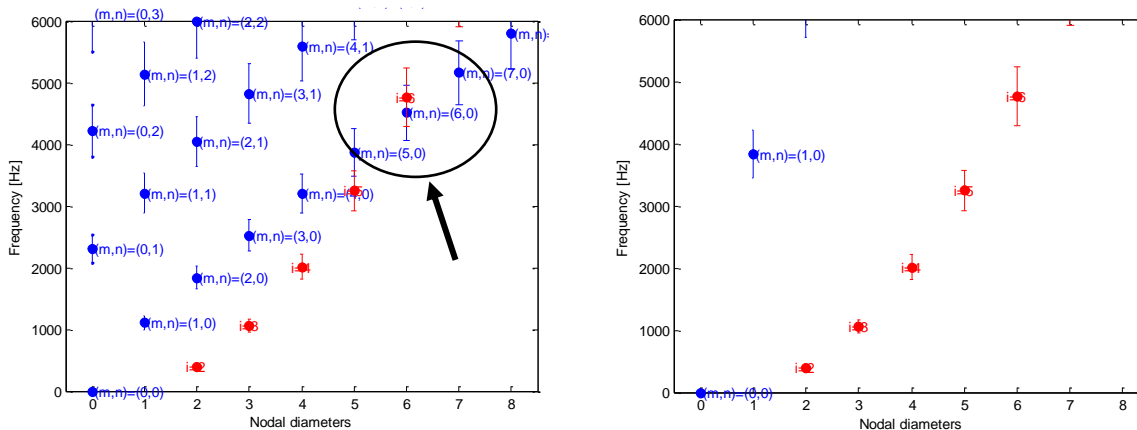


Figure 6-5. Typical interference diagram for LP system (8" line, 9 bara). Natural gas (left) and hydrogen (right). Blue dots are acoustic modes, red dots are structural modes. Coincidence risks is more prominent for natural gas than for hydrogen.

## 6.5 Conclusion

At similar energy transport rates, hydrogen seems to have more potential for acoustics-induced vibration (AIV) than natural gas. However, whether the increased levels in excitation energy effectively lead to pipewall vibration seems more unlikely, due to the limited chance of coincidence between acoustic resonant modes and structural pipe shell modes. Due to these opposing effects, it is concluded that the risk on AIV remains similar to the case with natural gas. Known practices to design and analyze the AIV phenomenon remain valid.

In all pressurized parts of the network where safety relief valves are in place, it is recommended to apply a screening (e.g. using [15]), in case of a transition to hydrogen. This will highlight areas with a potential risk and allows for a systematic review of re-design options (control of flow rates, replacement of orifice, mechanical modifications).

It is recommended to analyze in detail the results of a test conducted in 2020 on a district station [19]. Based on this analysis, the risks for fatigue failure in the LP network may be assessed in a more generic way.

## 7 Flow Induced Noise

### 7.1 Flow induced noise in natural gas transport systems

Natural gas transport systems need to be able to deliver gas without radiating too much noise to the environment. Noise exposure to the working personnel and to the environment is a critical aspect of the license-to-operate. Excessive noise emission is avoided, even if they are the result of incidental operations (e.g. venting). Whereas concerns related to noise are often connected to machinery (e.g. in the vicinity of compressor stations), also in intermediate assets as well as delivery locations and homes, noise has to be limited. A second important source of noise are pressure letdown (reduction) devices, and they are the most important sources downstream of the GTS system, in the RTL and RNB systems. Especially in the vicinity of households, noise generated in the pipes is also relevant, which happens at locations with concentrated pressure loss, such as elbows and T-pieces.

Pressure reduction devices are found at various locations within the transport system. For example, at the interface from the HTL to the RTL (the *Meet & Regel* stations M&Rs), pressure is reduced from 60 bar(g) to typically 40 bar(g). At the interface between the RTL and the RNB systems (Gas Ontvangst Stations, GOS) pressure is reduced to typically 8 bar(g). Where RNB systems dispatch gas to consumers at district stations, pressure is further reduced from typically 8 bar(g) to 100 mbar (g). Another example is at gas transfer stations (overslag stations), reducing from 8 bar(g) to 4 bar(g) (or even 1 bar(g)).

A few specific examples of pressure reduction devices that will generate noise:

- Pressure and flow control valves, for continuous operation. These are found in measuring and control station (M&R), gas receiving stations (GOS) and district stations.
- Pressure and flow control valves for semi-continuous operation. These are found in compressor stations, as compressor recycle valves and compressor anti-surge valves. These can also be found during extraction from high-pressure gas storage.
- Pressure reduction devices in incidental operation. These are found upon system pressurization and depressurization. These include blow-down valves and restriction orifice plates (single-hole or multi-hole). Also discontinuities in the low-pressure vent system may be locations with a large pressure reduction and high noise generation (T-joints, stack exit).

It is essential to understand that the noise perceived by an observer standing in the vicinity of the equipment is the result of (i) the magnitude of the acoustic sources in the fluid system creating noise *inside* the pipes, and (ii) the amount of energy that the pipes walls can radiate as they had become the diaphragm of a loudspeaker. This is illustrated in Figure 7-1. Therefore, in this chapter, the source of noise (and its magnitude) is treated separately from the radiation efficiency of the pipe walls.

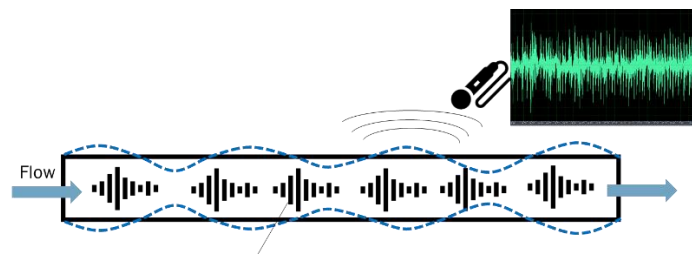


Figure 7-1. Schematic showing that the noise recorded by a microphone next to a pipe is the result of air pressure fluctuations caused the pipe wall vibrations, which are excited by the noise levels present in the gas flow as a result of different aerodynamic sources.

The negative consequences of the noise generation can be summarized as follows:

- Integrity issues, due to acoustic loading of the downstream mechanical structure. In particular at locations of ‘circumferential discontinuity’, such as small branch connections, T-joints and welded pipe supports, fatigue failures may occur. See chapter 6.
- Radiated noise, due to break-out of the in-line noise via the pipe wall. The break-out noise depends on the properties of the noise sources and on the properties of the pipe wall and installation details.
- Radiated noise, due to direct radiation from a vent stack. In industrial flaring systems, stack noise during depressurization may be a critical point in the environmental license to operate.
- Disturbance of flow metering equipment. For example, ultrasonic flowmeters installed closely downstream of a pressure reduction may be disturbed by (high-frequency) valve noise.

## 7.2 Assessment of flow-induced noise

### 7.2.1 Source: pressure reduction devices

In pressure reduction devices, the pressure is abruptly reduced. In general, noise amplitude increases with increasing mass flow and with increasing pressure differential. Other thermodynamic fluid properties generally have a smaller effect. The peak frequency depends on gas conditions but also on the dimensions of the turbulent contraction of the flow. The smaller the length scales in the pressure let-down device, the higher the frequency range. The intense generation of in-line noise in the process gas is most relevant at the downstream side of the source. In particular in choking conditions (when pressure differential  $P_{in}/P_{out}$  is sufficiently, typically  $\sim 2$  for natural gas) the noise will not propagate to the upstream side of the valve.

In the case of noise radiation, information about the noise frequency spectrum is essential. The prediction in AVIFF [15] does not allow for frequency evaluation of the noise. The IEC standard 60534-8 “Control valve aerodynamic noise prediction” [17] offers a detailed basis for estimation of source strengths. The physical background of this standard requires an advanced knowledge of gas dynamics and acoustics. However, the application of the prediction method is relatively straightforward. Operating conditions and gas parameters are required as input, as well as geometrical input, such as the dimension of the restrictions.

### 7.2.2 Source: pipes and flow fittings

Noise is generated by a fluid convected in a pipe as a result of turbulent structures arising near the walls of the pipe and in flow discontinuities, such as elbows or T-pieces. The energy dissipated in turbulence and noise is related to the pressure drop and therefore to the kinetic energy of the flow. This topic has been subject of research for a long time. A widely accepted reference whose foundations are also embedded in the AVIFF guidelines is that of Norton & Bull [20]. This reference contains experimental measurements of flow-induced noise for a variety of flow fittings and operating conditions, and suggests useful scaling laws. In particular, it provides a dimensionless power spectral density  $\phi_p$  of the pressure fluctuations (noise spectrum) as a function of dimensionless frequency for several geometrical configurations and different Mach numbers. The spectrum for a given case  $\Phi_p$  can be obtained by scaling the dimensionless function  $\phi_p$  with the velocity  $U$ , the fluid density  $\rho$  and the inner diameter  $d_i$ .

$$\Phi_p = \frac{\phi_p U}{\left(\frac{1}{2}\rho U^2\right)^2 \frac{d_i}{2}} \quad (\text{eq. 21})$$

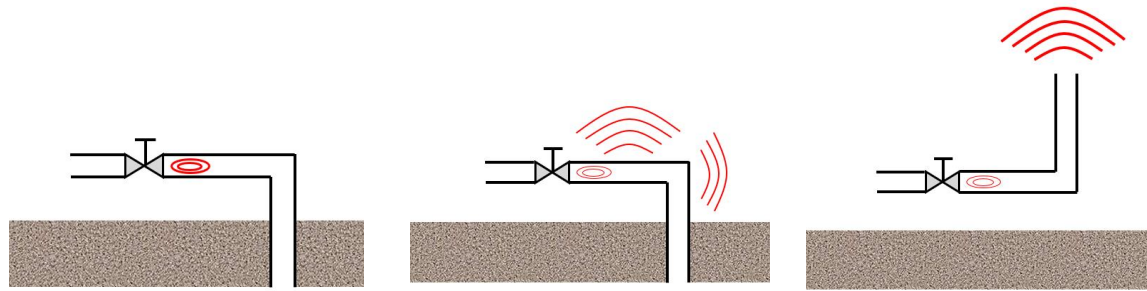


Figure 7-2. In-line noise generation (left), break-out noise through pipe wall (middle) and direct noise radiation from open stack (right).

### 7.2.3 Radiation

In external noise legislation, the noise exposure is quantified in terms of A-weighted noise levels. The A-weighting is a frequency filtering of the noise spectrum, which takes into account the sensitivity of the human ear. The human ear is relatively insensitive to low frequencies (< 500 Hz) and to very high frequencies (>8 kHz). The A-weighting is a standardized curve, shown in Figure 7-3. The A-weighting is a relevant aspect for the transition from natural gas to hydrogen, since the in-line noise sources have an upward frequency shift. If the existing noise source (natural gas) are dominated by frequencies around a few hundred Hertz, the upward frequency shift (hydrogen) results in noise in the ‘sensitive’ area of human observers. This has a non-favourable effect on the noise levels in dB(A). This situation may be expected in the high-pressure, high-capacity systems. If the existing noise source (natural gas) are dominated by frequencies around a few kHz, the upward frequency shift (hydrogen) results in noise in the ‘insensitive’ area, potentially even inaudible. This has a favourable effect on the noise levels in dB(A). This situation may be expected in the low-pressure, low-capacity systems (e.g. district stations and household and industrial consumers).

The in-line noise sources will propagate through the pipe wall and will be radiated from the wall (break-out noise). This interaction between inline noise, propagation through the pipe wall and radiated from the wall is an extremely complex process to model accurately. Moreover, the results may depend strongly on the details of the in-line noise, the pipe wall and installation effects. Similar to the practical modelling approach for the sources, also for the noise propagation information can be found in industrial standards. The VDI 3733 standard “Noise at pipes” [21] presents a practical and conservative approach for prediction break-out noise. A similar approach is also found in IEC 60534-8 [17].

Considering the broadband nature of the in-line noise source, the approach in broad frequency bands is considered most realistic. The transmission loss through the pipe wall has two separate contributions (the factor C is constant and depends on the installation details):

$$R_R = 10 \log \frac{c_R \rho_R s}{c_F \rho_F d_i} + A(f) + C \quad (\text{eq. 22})$$

The first term on the right-hand side depends only on the ‘impedance mismatch’ between the process fluid (subscript “F”) and the pipe material properties (subscript “R”) and the geometrical properties of the pipe wall (wall thickness  $s$  and diameter  $d_i$ ). For the transition to hydrogen, this ‘mass’ term results in a more favourable transmission loss: the impedance difference between hydrogen and the pipe wall is larger, and this will result in a transmission loss increase of typically +5 dB. This incremental effect applies to both steel pipes as well as plastic materials (HDPE or PVC).

The second term  $A(f)$  is a frequency-dependent function which represents the interaction with the ring frequency  $f_r$ :

$$f_r = \frac{c_R}{\pi d_i} \quad (\text{eq. 23})$$

At the ring frequency, exactly one structural wavelength fits in the circumference of the pipe. At this condition, the coupling to the pipe wall is optimal and the transmission loss is minimal. For frequencies below and above the  $f_r$ , the transmission loss increases, with different slopes:

$$\text{For } f \leq f_r : A(f) = 20 \log \frac{f_r}{f} \quad (\text{eq. 24})$$

$$\text{For } f > f_r : A(f) = 30 \log \frac{f_r}{f}$$

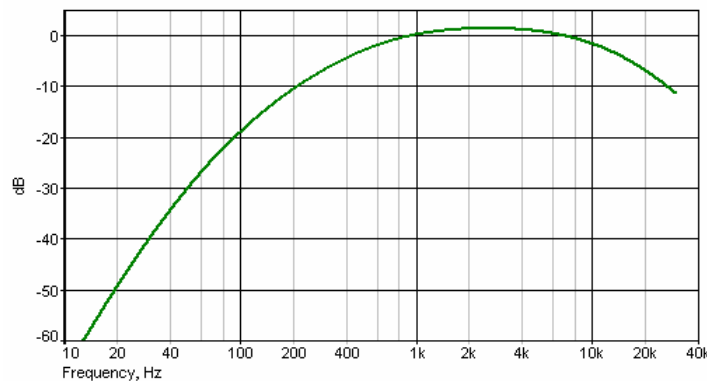


Figure 7-3. A-weighting curve, suppressing the contribution at the lower (<500Hz) and higher (>8kHz) frequencies.

## 7.3 Benchmark between natural gas and hydrogen

### 7.3.1 Source: pressure reduction devices

The basis of the benchmark is the same as discussed in section 6.3, but using the IEC method mentioned in the previous section. It is not possible to perform generic analysis of the source characteristics that includes all conditions of pressure and temperature as performed in other chapters of this report. Therefore, the benchmark for the source is based on multiple examples. The difference in actual noise source level and frequency between hydrogen and natural gas is quantified with the IEC standard for various typical configurations. It is stressed for clarity that this section is concerned with the magnitude of noise sources, i.e. levels experienced *inside* the pipe, and not the noise perceived by observers, i.e. experienced *outside* the pipe. The following example cases were considered:

- Blow-down of compressor station
- Measuring and control station
- Gas receiving station
- Gas district station
- Households and industrial consumers

#### 7.3.1.1 Example Case 1: blow-down compressor station vent

This case is a typical high-pressure, high-capacity blowdown system on a compressor station (HTL system), with incidental operation. The upstream pressure is varied from 50 bar to 80 bar(a), with a

constant backpressure of 3 bar(a) downstream of the blow-down orifice. The dimensions of the blow-down orifice are based on an actual field case of a compressor station main vent. The vent maximum capacity is approximately 147 kg/s or 637 kNm<sup>3</sup>/h (values for natural gas). The bore of the restriction is kept constant for natural gas and hydrogen.

The results for the sound power level of the source are shown in Figure 7-4. The sound power level for hydrogen is 5-6 dB higher than for natural gas. The offset is constant for the various pressure conditions. The results for the peak frequency of the source are shown in Figure 7-5. The peak frequency for hydrogen is a factor 3.2-3.3 higher than for natural gas and shifts towards frequencies in which humans are more sensitive to noise. The ratio is constant for the various pressure conditions.

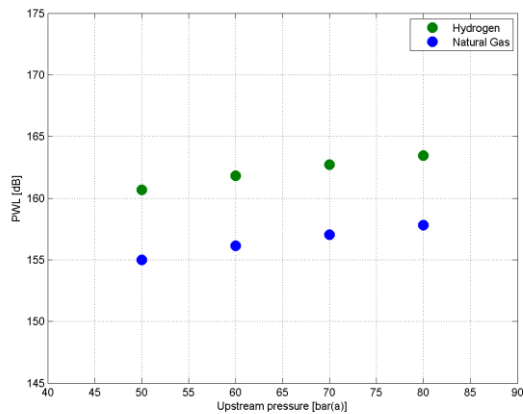


Figure 7-4. Sound power level of blow-down orifice noise source inside the pipe, for hydrogen and natural gas.

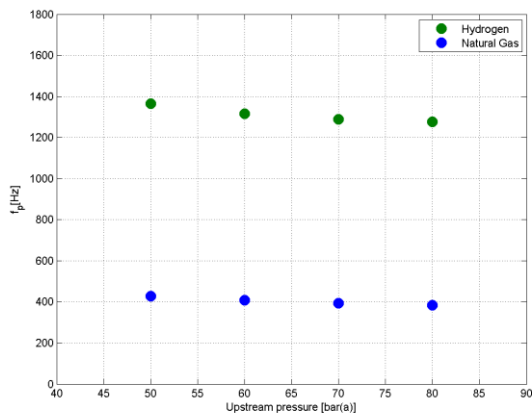


Figure 7-5. Peak frequency of blow-down orifice noise source inside the pipe, for hydrogen and natural gas.

### 7.3.1.2 Example Case 2: measuring and control station

This case is a typical high-pressure, high-capacity configuration, with continuous operation. The station inlet pressure is varied from 80 bar(a) to 50 bar(a), with a constant outlet pressure of 40 bar(a). The dimensions of the contraction in the control valves are based on a realistic, large capacity of 510 kNm<sup>3</sup>/h (values for natural gas).

The results for the sound power level of the source are shown in Figure 7-6. The sound power level for hydrogen is 6-8 dB higher than for natural gas. The offset is relatively constant for the various pressure conditions. The results for the peak frequency of the source are shown in Figure 7-7. The peak frequency for hydrogen is a factor 3.2-3.5 higher than for natural gas. The ratio is relatively constant for the various pressure conditions. Without taking into account eventual radiation properties of the pipe (explained in the next section), this would mean higher noise levels towards frequencies in which the human ear is more sensitive to. Note that the source sound power level is lower than for the Case 1, due to the lower pressure ratio over de valve resulting in lower acoustic efficiencies. No noise reduction due to a possible low-noise trim design of the control valve is accounted for in these results.

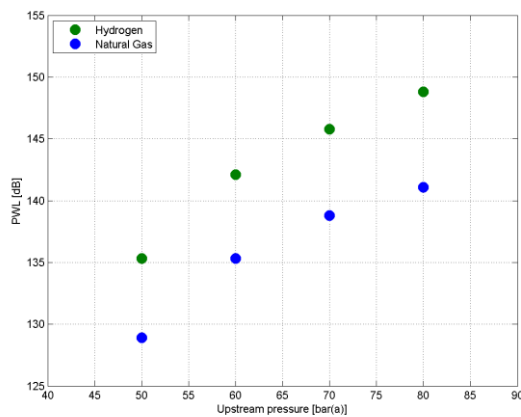


Figure 7-6. Sound power level of control valve noise inside the pipe, for hydrogen and natural gas.

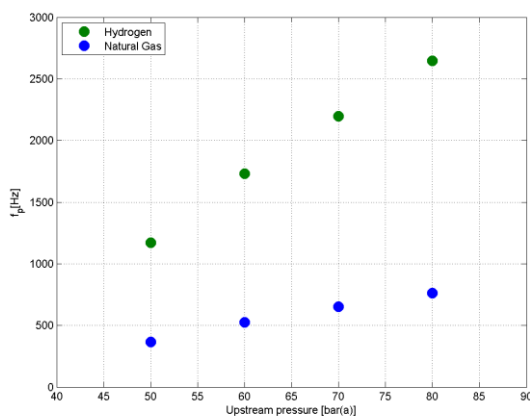


Figure 7-7. Peak frequency of control valve noise inside the pipe, for hydrogen and natural gas.

### 7.3.1.3 Example Case 3: gas receiving station

This case is a typical medium-pressure, medium-capacity configuration, with continuous operation. The station inlet pressure is varied from 50 bar(a) to 30 bar(a), with a constant outlet pressure of 9 bar(a). The dimensions of the contraction in the control valves are based a realistic, large capacity of 42 kNm<sup>3</sup>/h (values for natural gas).

The results for the sound power level of the source are shown in Figure 7-8. The sound power level for hydrogen is 5-6 dB higher than for natural gas. The offset is constant for the various pressure conditions. The results for the peak frequency of the source are shown in Figure 7-9. The peak frequency for hydrogen is a factor 3.1 higher than for natural gas. For natural gas, the frequency is around 2 kHz and for hydrogen between 6 - 7 kHz. The human ear is most sensitive to the frequency spectrum between 1-9 kHz. The frequency shift has no significant influence on the sensitivity. The ratio is constant for the various pressure conditions. Note that the absolute source sound power level is lower than for the Case 1, due to the lower pressure ratio over de valve resulting in lower acoustic efficiencies. No noise reduction due to a possible low-noise trim design of the control valve is accounted for in these results. Also note that the absolute frequencies are much higher than for Case 1, which is a consequence of the smaller dimensions of the control valve restriction (lower capacity).

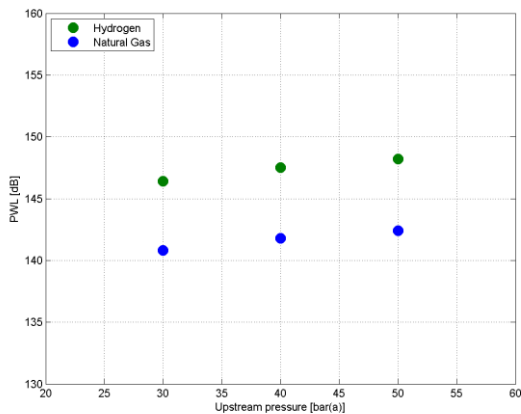


Figure 7-8. Sound power level of control valve noise inside the pipe, for hydrogen and natural gas.

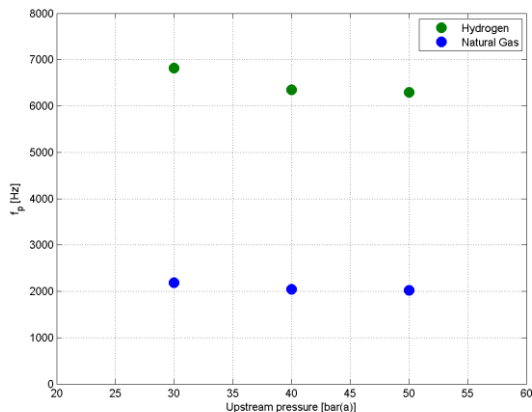


Figure 7-9. Peak frequency of control valve noise inside the pipe, for hydrogen and natural gas.

### 7.3.1.4 Example Case 4: gas district station

This case is a typical low-pressure, low-capacity configuration, with continuous operation. The station inlet pressure is varied from 11 bar(a) to 3 bar(a) (notice that 9 bar(a) is the actual maximum and 2 bar(a) is the actual minimum), with a constant outlet pressure of 100 mbar(g). The dimensions of the contraction in the control valves are based a realistic capacity of 4000 Nm<sup>3</sup>/h (values for natural gas).

The results for the sound power level of the source are shown in Figure 7-10. The sound power level for hydrogen is 5 dB higher than for natural gas. The offset is constant for the various pressure conditions. The results for the peak frequency of the source are shown in Figure 7-11. The peak frequency for hydrogen is a factor 3.0-3.1 higher than for natural gas. For natural gas, the frequency is around 2 kHz and for hydrogen between 6 - 7 kHz. The human ear is most sensitive to the frequency spectrum between 1-9 kHz. The frequency shift has no significant influence on the sensitivity. The ratio is constant for the various pressure conditions. Note that the absolute source sound power level is lower than for the Case 1, due to the lower pressure ratio over de valve resulting in lower acoustic efficiencies. No noise reduction due to a possible low-noise trim design of the control valve is accounted for in these results. Also note that the absolute frequencies are much higher than for Case 1, which is a consequence of the smaller dimensions of the control valve restriction (lower capacity).

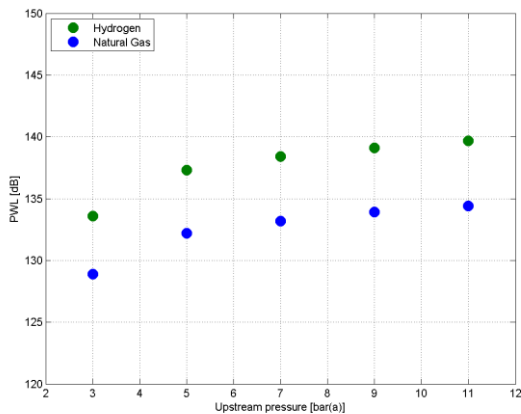


Figure 7-10. Sound power level of control valve noise inside the pipe, for hydrogen and natural gas.

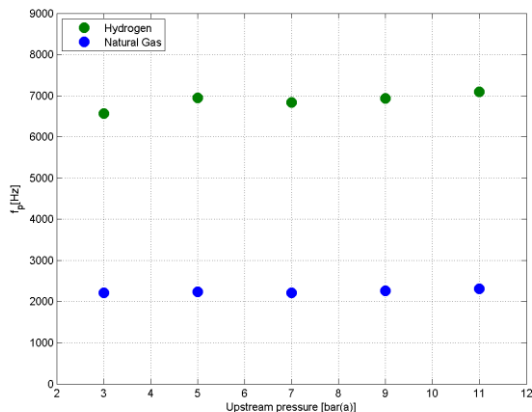


Figure 7-11. Peak frequency of control valve noise inside the pipe, for hydrogen and natural gas.

7.3.1.5 Example Case 5: households and industrial consumers

This case is the final pressure reduction in the gas supply chain. The nominal inlet pressure is 100 mbar (g), but could be up to 1 bar(g), the outlet pressure being atmospheric. The dimensions of the contractions are estimated, based on a maximum capacity of 10 Nm<sup>3</sup>/h (G6, households) and 400 Nm<sup>3</sup>/h (industrial consumers). Note that these values are upper worst-case limits. A realistic estimate for the nominal (high) value of a household is up to 2 Nm<sup>3</sup>/h, which would result in much lower noise amplitudes.

The results for the sound power level of the source are shown in Figure 7-12. The sound power level for hydrogen is 4-5 dB higher than for natural gas. The offset is constant for the various pressure conditions. The results for the peak frequency of the source are shown in Figure 7-13. The peak frequency for hydrogen is a factor 3 higher than for natural gas, which may shift it towards inaudible frequencies to humans. The ratio is constant for the various pressure conditions. Note that the absolute source sound power levels are much lower than for the Case 1, due to the lower pressure ratio resulting in lower acoustic efficiencies. Also note that the absolute frequencies are much higher than for Case 1, which is a consequence of the smaller dimensions of the restriction (lower capacity).

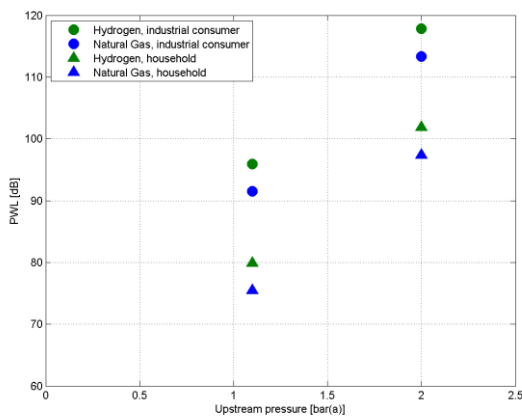


Figure 7-12. Sound power level of control valve noise inside the pipe, for hydrogen and natural gas.

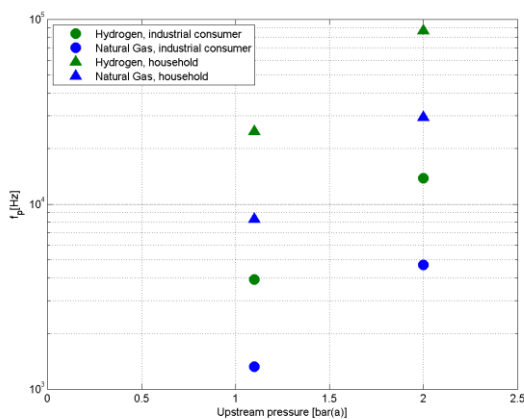


Figure 7-13. Peak frequency of control valve noise inside the pipe, for hydrogen and natural gas.

### 7.3.2 Source: pipe and flow fittings

In the case of noise generated in pipes and flow fittings, quantification of the difference between hydrogen and natural gas relies on (eq. 21). According to this equation, the outcome depends on the flow velocity ratio and the dynamic pressure ratio (squared) for a given geometry. Therefore the results shown in Figure 2-3 and Figure 2-5 can be combined to conclude that hydrogen is expected to feature 3-4 times more energetic pressure fluctuations than natural gas transporting the same amount of energy.

This is further elaborated with an example for the noise generated in a straight pipe. The parameters for this example are not very important as the flow velocity ratio and the dynamic pressure ratio are not extremely sensitive to pressure and temperature. Figure 7-14 shows the difference in power spectral density for hydrogen and for natural gas. The plot presents in a log-log scale the frequency spectrum for both cases, with hydrogen featuring a concentration of energy at larger frequencies than natural gas. It is noted that the overall power level of this spectrum is about 3 times larger for hydrogen than for natural gas (despite the general appearance of the plot due to the log scale).

Though the spectra look different for other geometrical configurations, such as long-radius elbows and T-pieces, the general conclusions of the benchmark between hydrogen and natural gas remain the same.

### 7.3.3 Noise radiation

The quantification of noise radiation is explored using the VDI method described in 7.2.3. To determine the impact of the transition to hydrogen on  $A(f)$  in (eq. 22), one must know the frequency range of interest of the source and compare this with the ring frequency (depends on pipe material and diameter). The transition to hydrogen introduces an upward frequency shift. If the frequency range of interest is  $< f_r$ , then the transition to hydrogen results in an unfavourable transmission loss. If the frequency range of interest is  $> f_r$ , then the transition to hydrogen results in a favourable transmission loss. In case the frequency range of interest is overlapping with the  $f_r$ , it is not possible to make a general statement on the effect of transition to hydrogen.

Note that for non-metallic pipes which are used in the LP distribution networks (HDPE, PVC) the ring frequency tends to lower values, while the source frequencies are generally high (and shifting even higher in case of hydrogen). For these reasons, it is expected that in the LP part of the network with non-metallic pipes, the transmission loss for hydrogen will be favourable (favourable mass effect and favourable frequency effect).

Some of these features are illustrated in Figure 7-15. The frequency curves  $A(f)$  are plotted for various, typical line sizes and compared with the typical frequency range of the in-line noise source. The upward shift in source frequency (natural gas  $\rightarrow$  hydrogen) is obvious in both figures. For the left figure (HP Case 1, with steel pipes), the source frequencies for hydrogen shift into the 'un-favourable' frequency range around  $f_r$  and have hence a poor transmission loss. For the right figure (LP Case 4, with HDPE pipes), the source frequencies for hydrogen shift away from the 'un-favourable' frequency range and have hence a better/higher transmission loss.

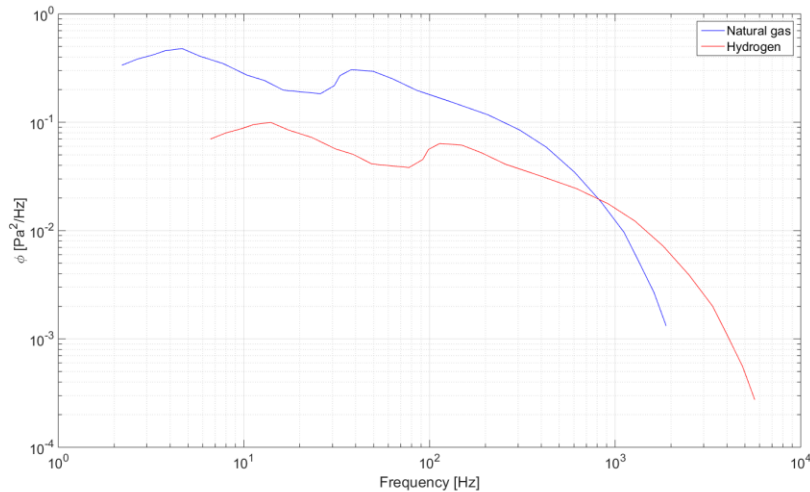


Figure 7-14. Power spectral density of hydrogen and natural gas as generated in a straight pipe under a given set of conditions. In this case, ( $ID = 150 \text{ mm}$ ,  $U_{NG} = 10 \text{ m/s}$ ,  $U_{H_2} = 30 \text{ m/s}$ ,  $80 \text{ bar}$  and  $10 \text{ deg. C}$ ).

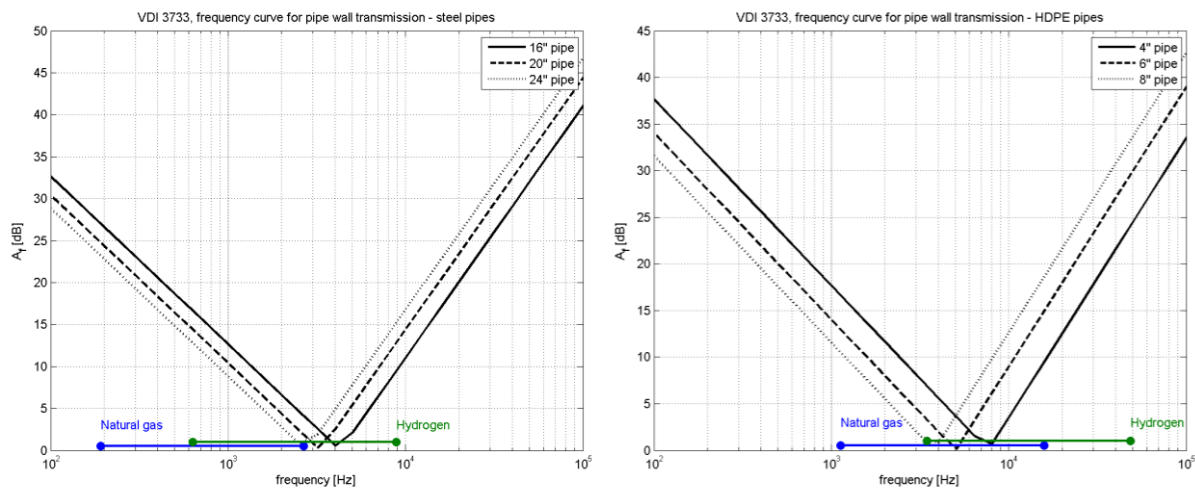


Figure 7-15. Transmission loss frequency function  $A(f)$ . Left: high-pressure, large-capacity blowdown system (CASE 1). Right: district station (CASE 4).

### 7.3.3.1 Noise radiation through open stacks

As for the break-out noise through the pipe wall, also the acoustic radiation from an open stack involves various physical mechanisms. The acoustic attenuation of the noise is depending on the frequency, and will be favourable for the upward frequency shift in case of hydrogen. Also, in case of an outlet silencer at the stack, it is expected that the performance of absorptive types silencers is more favourable for the case of hydrogen. On the other hand, the noise radiation from the stack exhaust may be stronger for higher frequencies.

For a quantitative statement, a detailed assessment on a case-by-case basis will be needed.

Preliminary tests with blow-down of a low-pressure distribution network confirm that no noticeable increase in radiated noise is observed, in case of hydrogen [22].

## 7.4 Conclusion

Noise is generated as a byproduct of flow. Wherever flow energy is lost (pressure drop), sources of noise arise. This occurs in normal, straight pipes due to friction, and any other flow fittings in which pressure is lost. This phenomenon is much more visible in pressure let-down devices such as control valves and restriction orifices. Based on the discussion above, it is expected that sources of noise with hydrogen tend to become stronger. Frequencies shift to higher values, which can be beneficial. Also, the radiation characteristics of typical pipes tend to be favourable to hydrogen. The current limited benchmark experience with hydrogen confirms that less noise was radiated to the environment [19]. At this stage, though, it is too early to generalize the conclusion that less noise will be radiated from hydrogen systems than from natural gas systems.

Base on the examples presented in this chapter, the following conclusions have been reached:

- With a transition from natural gas to hydrogen, noticeable effects are expected on the mechanism of valve noise generation. A systematic increase in noise source strength (4-8 dB) is predicted, using comprehensive prediction methods [17]. A systematic upward shift in frequency is expected, of approximately a factor 3.
- Noise radiation from the pipe wall (break-out noise) contains various aspects, such as the expected frequency range of the source and the mechanical properties of the pipe. In any case, a systematic beneficial effect of approximately 5 dB is found for hydrogen, due to the increased impedance mismatch between process gas and pipe wall. On the other hand, the frequency effect of the pipe wall transmission loss depends on the pipe dimensions, the pipe material and the frequency range of the noise source. This frequency effect could be positive, neutral or negative. Evaluation at future, actual operating conditions with hydrogen is recommended.
- Also, the quantitative assessment of noise radiation from an open stack should be done on a case-by-case basis.

In order to better understand what effects are dominant, more experimental evidence around the subjects discussed above is required. Particularly, experience at very high pressure typical of the HTL system is missing. Ongoing experimental campaigns with flowing hydrogen should include suitable environmental noise measurements, whether in the GTS, the RNBs or the household levels. These measurements should be reproduced with existing modelling techniques, with the objective to more confidently extrapolate the use of such models to any other locations and conditions. An example of this is the campaign reported in reference [19].

Finally, it is reminded that in the close vicinity downstream of the pressure reduction devices, flow meter accuracy may be disturbed by the increased noise. This phenomenon is excluded from the scope of this HyDelta WP1E and is recommended for further research.

## 8 Erosion

### 8.1 Erosion in natural gas transport systems

Erosion is defined as the process by which material is worn away from the gas transport system due to the impact of particles transported in the flow. Erosion typically causes thinning of pipes at particular hot spots and overall physical degradation of equipment.

Erosion is a well-known integrity risk in the oil & gas industry, such that erosion probes even exist in many upstream assets. Erosion can be the limiting factor for the maximum flow velocity possible in the pipework and thus become an important design constraint. The eroding agent is in most cases solid sand produced together with the hydrocarbon stream. Liquid droplets are not considered a potential abrasive agent at flow velocities below 70 - 80 m/s [23], which in gas transport systems (including future service with H<sub>2</sub>) are not reached. Erosion, on the other hand, is not known to pose a significant risk to the integrity of gas transport systems (of The Netherlands). This is because prior to injection in the GTS, gas has been treated and cleaned. Furthermore, intermediate gas receiving stations (GOS) incorporate filters to capture incidental ingress of solids or rust particles shed anywhere in the system. It is possible though that in incidental events, solid particles enter the network, which can eventually lead to issues with combustion in domestic boilers [24].

According to NBNL, wall thickness measurements are performed in the HP RNB system (1-8 barg) when, for example, side branches need to be added to the network. Even though the pipes could be as old as 50 years, no loss of material has been observed. In the LP RNB system (0.1-1 barg), visual inspections conducted with cameras indicate that the system can contain more contamination, with twigs, leaves, and other bodies present. However, there is no documentation of this creating erosion issues, partially explained by the fact that the flow velocity is lower. It cannot be excluded that if the flow velocity in the LP RNB system was as high as 20 m/s, erosion issues would not arise.

Therefore, the starting point for erosion as a failure mechanism is that it currently does not create integrity concerns (either because of the absence of foreign particles or because the speeds are far below the limit of 20 m/s). It is of interest though to understand whether service with high-speed hydrogen can affect the level of risk associated to the erosion phenomenon.

### 8.2 Assessment of erosion

In the upstream sector, erosion is normally taken into account as part of designs compliant with API RP 14E [25]. For single phase gas lines, in fact the main factor constraining the design would be the pressure drop. It has been argued in general that the approach proposed by API 14E is not holistic and important interactions between erosion and possible corrosion are missed [26]. An additional widely used document is the DNV recommended practice O501 [27]. This document provides a more fundamental approach to characterizing erosion rates. The actual loss of material  $E_m$  [kg/s] can be estimated from:

$$E_m = K U_p^n F(\alpha) m_p \quad (\text{eq. 25})$$

Where  $K$  [m/s<sup>-n</sup>] and  $n$  are coefficients dependent on the pipe material,  $U_p$  is the particle impact velocity [m/s], and  $m_p$  [kg/s] is the loading of solid particles that the flow is transporting. The function  $F(\alpha)$  corresponds to a correction factor for the particle impact angle  $\alpha$  and the ductility class of the material.

In order to assess erosion rates, several workflows can be followed in ref. [27], applicable to different geometries to be assessed, such as straight pipe, elbows, reducers or control valves. Values for

different, common materials are found in the reference. Regardless of the workflow followed, the conclusions when comparing natural gas to hydrogen will be similar, so the scope of this document is limited to the assessment of elbows.

### 8.3 Benchmark between natural gas and hydrogen

When comparing natural gas to hydrogen flow, the following assumptions have been taken:

- Hydrogen transporting the same amount of energy as natural gas.
- Pipes made of steel, HDPE and PVC.
- Erosive agent: sand.
- Solid loading: maximum as per Ministeriële Regeling *Gaskwaliteit* [28].

By examination of (eq. 25), it is observed that the only parameter that is directly connected to the flow is the particle impact velocity. At sufficiently high flow velocities, solid particles will be lifted and transported with the flow (in equilibrium). In this situation, the particle impact velocity is the gas flow velocity. For instance, for steel the value of the parameter  $n$  is 2.6. The sensitivity to gas velocity is illustrated in Figure 8-1. Assuming every other parameter constant, it would mean that hydrogen flowing  $\sim 3$  times faster than natural gas would feature erosion rates roughly 17 times larger. There are other parameters though that depend on the flow, such as the impact angle for a given geometry or the pipe wall area potentially exposed to particle impacts. Therefore this ratio cannot be fully generalized.

A second difficulty in establishing a generic benchmark is that the maximum solid rate stated by the Gas Quality Law is given as  $100 \text{ mg}/(n)\text{m}^3$ . Because the composition of the gas can differ leading to different fluid densities at normal conditions, this means the actual maximum solid particle rate will differ when comparing different gas compositions. A comparison choice must be made: either the solid particle rate is calculated for the natural gas case and fixed when comparing to hydrogen, or the maximum limit according to the current legal framework is respected. This is illustrated in Table 8-1. In the former case the ratio between hydrogen and natural gas is  $\sim 17$ , in the latter case, it is nearly  $\sim 50$ . Because there is no particular reason to expect that pipes with hydrogen will contain more solids than those with natural gas, the case comparing similar solid rates is considered more realistic.

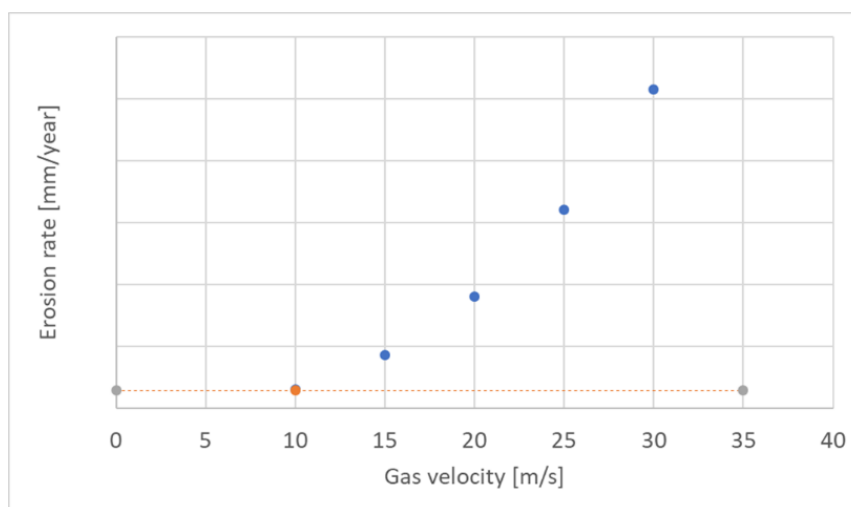


Figure 8-1. Erosion rate as a function of gas velocity in a given elbow configuration, according to sensitivity following  $U^{2.6}$ . The absolute numbers in the y-axis are removed due to material dependency, whereas it is the difference that is intended to be illustrated.

Table 8-1. Generic benchmark of erosion rate for natural gas and hydrogen illustrating that there is a significant difference between assuming the same amount of solids in both cases, or if in both cases the maximum current legal limit is followed.

	G-gas	Hydrogen
Max Solid rate [mg/(n)m <sup>3</sup> ]	100	100
Density at normal conditions [kg/(n)m <sup>3</sup> ]	0.833	0.089
Actual particle loading at normal conditions [mg/kg]	120	1120
Calorific value, LHV [MJ/kg]	38.02	119.96
Calorific value, LHV [MJ/(n)m <sup>3</sup> ]	31.67	10.71
Energy-specific flow rate [n(m <sup>3</sup> )/MJ]	0.032	0.093
Energy-specific solid rate [mg/MJ]	3.16	9.34
Flow velocity ratio at normal conditions [-]	n.a.	2.96
Solid rate ratio at normal conditions [-]	n.a.	2.96
Erosion rate ratio - assuming only same solid rate (steel)	16.8	
Erosion rate ratio - assuming same original legal limit (steel)	49.6	

## 8.4 Examples

In this section, a number of typical cases for the gas network of the Netherlands is used for illustration purposes. All calculations are based on ref. [27] in which the necessary material constants are also found. All apply to the case of a pipe elbow. The solid rate for the hydrogen case is the same as in the natural gas case, i.e. the maximum legal limit is only applied to the natural gas case, and the value obtained is used also for the hydrogen case. In all cases it is assumed that the solid rate is constant. In reality, possible pockets of solid particles will be convected through the network and erode a particular spot only for a limited amount of time. The cases (1-8) and parameters as used in the calculations are provided in Table 8-2.

The first observation is that, when 10 m/s is used as the baseline flow velocity of natural gas, erosion rates on an hourly basis are limited. Only if solid contamination was constantly present, it would lead to any visible erosion rates over the years. This may explain the current state of affairs in which erosion is not observed as an issue, which is partly explained by the use of preventive measures to limit solid contamination as well as the limit flow speed used in the gas networks. Switching to hydrogen at high speed would render much higher erosion rates. While this in general the dominant trend, the erosion potential can differ due to other parameters, e.g. due to the particle size being above or below a threshold limit determined by flow-related metrics (Reynolds number, fluid density). The model used features steep, discontinuous changes in behaviour depending on the aforementioned flow-related metrics. Results cannot be extended to the RNB system because the density of the fluid is lower than 1 kg/m<sup>3</sup>, which is outside of the application range of the model presented in ref. [27]. It is anticipated that erosion rates are also larger, but it cannot be confidently stated from this model alone. Follow-up research for the conditions typical of the RNBs is recommended.

Table 8-2. Parameter used in the calculations of absolute erosion rates. The solid particle loading in the hydrogen case is assumed constant for 1 full hour and the same as in the natural gas case (i.e. not based on applying the maximum legal limit to either case independently).

Case #	1	2	3	4	5	6	7	8
Pressure [bar(a)]	80	40	40	8	8	2	1.1	1.1
Pipe material (*)	steel	steel	steel	steel	HDPE	HDPE	HDPE	HDPE
Pipe Diameter [DN]	1200	1200	400	200	200	200	200	100
Material constant K [ $10^{-9}m/s^{-n}$ ]	2.0	2.0	2.0	2.0	3.5	3.5	3.5	3.5
Material exponent, n [-]	2.6	2.6	2.6	2.6	2.9	2.9	2.9	2.9
Material density [ $kg/m^3$ ]	7800	7800	7800	7800	1150	1150	1150	1380
Sand density [ $kg/m^3$ ]	2650	2650	2650	2650	2650	2650	2650	2650
Sand particle diameter [ $\mu m$ ]	100	100	100	100	100	100	100	100
Solid content [ $mg/(n)m^3$ ]	100	100	100	100	100	100	100	100
Flow velocity (G-Gas) [m/s]	10	10	10	10	10	10	10	10
<b>Results</b>								
Wall thickness loss (G-gas) [ $\mu m/h$ ]	0.0024	0.0021	0.005	0.0036	0.08	0.02	0.004	0.0001
Wall thickness loss (H <sub>2</sub> ) [ $\mu m/h$ ]	0.34	0.24	0.33	**	**	**	**	**
Erosion rate ratio [-]	141	117	60	**	**	**	**	**

(\*) Though it was possible to find information about erosion in PVC pipes, it has not been possible to confidently determine the numerical values that should be assigned to feed the empirical model of ref. [27]. (\*\*) Unfortunately the density of hydrogen at such pressures is below  $1 kg/m^3$ , which is outside the applicability range of the model used.

## 8.5 Conclusion

Erosion is currently not seen as an integrity risk in gas transport systems. There is no evidence of it being an issue even after decades of operation in The Netherlands. Gas cleaning processes and filters at different locations of the systems are in place to prevent this. Nonetheless, incidentally, limited amounts of solid particles will enter the network. When hydrogen is used to transport the same amount of energy as in natural gas systems, it is expected that the erosion potential for such particles is much larger. This is due mostly to the large effect that the flow speed has on the expected erosion rates.

Considering the above and the fact that other references point to erosion as a limiting factor creates enough grounds for follow-up research, and cooperation with other initiatives in Europe on this regard. Furthermore, the application range of the method selected to characterize erosion rates does not cover hydrogen flows at low pressures typical of the RNB systems. Follow-up research on erosion could scope:

- Erosion tests in the lab to characterize the materials used in the RNB systems.
- Verify the performance of the adopted model in comparison to simulations performed with computational fluid dynamics for typical flow fittings and pipe materials.
- Determination of worst flow velocities in the networks and worst-case duration to exposure to solid contamination by means of network simulations.

## 9 Perspectives and closing remarks

The flow velocity of a gas in a pipeline transport system is limited by a number of phenomena. The flow velocity is determined by the selection of system capacity, operating conditions, hardware sizing and other items not necessarily technical. The combination that provides the lowest levelized cost of transport determines what the resulting flow velocity is at all points of the transport system.

However, the flow velocity itself can be a constraint in this optimization due to the risks associated to very high speed flows. For natural gas, this limit is typically set at 20 m/s (72 km/h). If the same limit would be applied to hydrogen, it may be a conservative constraint on the capacity of new and re-used systems to transport energy.

The phenomena linked to integrity risks associated to high speed gas flows have been explored in this report. A generic benchmark between natural (G-) gas and hydrogen is presented, when an equal energy transport capacity between the two carriers is assumed. The objective of the benchmark is to evaluate whether under this assumption, any barriers prevent transport at such condition. In other words, whether the allowable flow velocity for hydrogen can be larger than the value traditionally used for natural gas or in which conditions that is allowed.

In this study, existing methods to quantify the risks associated to the phenomena involved are used. These are widely used across industry, not only in natural gas transport systems, but also in the upstream hydrocarbon production sector or the petrochemical industry. The methods are typically generic, and hydrogen is no exception. It must not be forgotten that hydrogen transport is already successfully done through thousands of kilometres of pipelines globally, though locally this may be done at rates and conditions less demanding than those envisioned now for the energy transition. For the purpose of the analysis of these phenomena, hydrogen is not different from natural gas or other gases. The Energy Institute guidelines [15] can be followed as usual for flow-induced integrity risks. Compressor equipment can be designed as usual against the API 618 standard. Erosion control guidelines such as API RP 14E or DNV RP O501 can also be followed.

The main result of this investigation is that the risk levels associated to these phenomena when hydrogen flows with the same energy rate as natural (G-) gas are similar. If with natural gas transport, 20 m/s is a rule of thumb for the maximum flow velocity in the network, 60 m/s could be the rule of thumb for hydrogen. Operation of hydrogen at the same flow velocity of 20 m/s will render a significantly milder situation from every aspect analysed in this report. Operation at 40 m/s may be equally possible although issues with thermowells start to appear and erosion potential is also already significantly increased. In order to achieve the flow velocity required for similar energy transport capacities between hydrogen and natural gas, two warnings must be indicated.

The first warning is connected to erosion potential. Gas transport pipelines are normally very clean and free of potentially eroding agents such as sand. Of course, in the absence of eroding agents, (internal) erosion can't exist. However, it has been concluded that should there be incidental ingress of sand, the eroding potential of high speed (hydrogen) flows is dramatically increased. Whether filters perform as well as with natural gas, and whether stricter maintenance is warranted is currently uncertain. It is important to explore the performance of filters in the GTS and RNB systems with high speed hydrogen flow. It is equally important to define worst-case exposure to solid particles. This should enable a better quantification of the risk of solid contamination in the gas stream responsible for potential erosion. A second line of research can be linked to dedicated flow simulations to characterize worst-case erosion rates in the RNB systems, in combination with suitable material constants for PVC pipes, for which tests may be required.

A second, milder warning arising from these investigations is linked to dynamics at high frequencies. Even in the case that hydrogen presents comparatively lower pulsation or radiated noise amplitudes than natural gas, it will do so at 3 times higher frequencies. From a mechanical vibration mitigation perspective, that may be more difficult to achieve, even for lower amplitudes. The same holds for noise: whereas in some cases, higher frequencies will render either better blockage from the pipe or even moving beyond (human) audible range, the opposite could also be true: that the pipe is more transparent and will radiate more noise, and that it may be at frequencies that humans are more sensitive to. It is unfortunately not possible to generalize what the dominant trend will be, so each case must still be assessed in a case-by-case basis. This is anyway standard practice in industry even with natural gas transport assets or other industrial processes, so it is not considered a critical aspect demanding additional research and caution. Existing risk quantification and mitigation methods are valid and should be applied.

Some of the conclusions presented herein should be checked in field tests. For example, noise generation and radiation in gas district stations has been successfully checked in 2020 in cooperation with the same HyDelta partners [19]. When possible, it is recommended to look after phenomena described in this report in field tests involving flowing hydrogen. That would provide the end evidence to ascertain the trends and conclusions observed in this report.

A final note is made with respect to subjects currently not in the scope of this report. Possible metering errors in flow meters as a result of unsteady flows (pulsations, turbulence) should be better understood, which is an aspect also linked to the flow speed. It is recommended to explore these phenomena as an integral part of the investigations conducted to determine the requirements for flow metering equipment for hydrogen service.

## 10 List of References

- [1] Gasunie Transport Services, *Ontwerp Uitgangspunten transportsystemen*, 1 7 2014.
- [2] NEN, *7244 - Gasvoorzieningsystemen - Leidingen voor maximale bedrijfsdruk tot en met 16 bar*, NEN, 2014.
- [3] NEN, *3650 - Transportleidingen*, NEN, 2020.
- [4] NEN, *1059 - Gasvoorzieningsystemen - Gasdrukregel- en meetstations voor transport en distributie*, NEN, 2019.
- [5] Netbeheer Nederland, *Handleiding Nestor Gas, versie 4.0*, 1 1 2018.
- [6] NEN, *3651 - Aanvullende eisen voor buisleidingen in of nabij belangrijke waterstaatswerken*, NEN, 2020.
- [7] ASME, *B31.12 Hydrogen Piping and Pipelines*, American Society of Mechanical Engineers, 2020.
- [8] N. González Díez, S. van der Meer, J. Bonetto and A. Herwijn, *Technical assessment of Hydrogen transport, compression, processing offshore*, North Sea Energy, 2020.
- [9] HIGGS project, <https://www.higgsproject.eu/the-project/>, 2021.
- [10] H21 project, *H21 Strategic Modelling Major Urban Centers*, 2021.
- [11] K. Steiner, *20 m/s – über die Strömungsgeschwindigkeiten in der Gasinfrastruktur*, 2021.
- [12] N. Albers, L. van Lier and M. van der Biezen, "Engineering approach for world's largest hydrogen compression system," in *11th EFRC Conference*, Madrid, 2018.
- [13] Wikipedia, *Energy Density*, [https://en.wikipedia.org/wiki/Energy\\_density](https://en.wikipedia.org/wiki/Energy_density), (Accessed on February 26, 2019).
- [14] KIWA, *Toekomstbestendige gasdistributienetten*, Apeldoorn: KIWA, 2018.
- [15] Energy Institute, *Guidelines for the Avoidance of Vibration Induced Fatigue Failure in Process Pipework*, 2008.
- [16] ASME *PTC 19.3 TW-2016 - Thermowells*, American Society of Mechanical Engineers, 2016.
- [17] IEC 60534-8, *Industrial process control valves - Part 8-3: Noise considerations - Control valve aerodynamic noise prediction method*, 2011.
- [18] NORSOK, *L-002 Standard - Piping system layout, design and structural analysis, 4th edition*, 2016.
- [19] C. Lock, *Gasdrukregelstation voor waterstof*, Apeldoorn: Kiwa N.V., 2020.

- [20] M. Norton and M. Bull, "Mechanisms of the generation of external acoustic radiation from pipes due to internal flow disturbances," *Journal of Sound and Vibration*, vol. 1, no. 94, pp. 105-146, 1984.
- [21] VDI 3733, *Noise at pipes*, 1996.
- [22] Netbeheer Nederland, *Affakkelen en afblazen van waterstof (KIWA)*, 2021.
- [23] N. Barton, *Erosion in Elbows in Hydrocarbon Production Systems: Review Document*, Glasgow: TÜV NEL Ltd for HSE Executive, 2003.
- [24] A. Kooiman, "Stof tot nadenken," *Gasnet*, vol. 32, no. 2, June 2018.
- [25] American Petroleum Institute, *API RP 14E : Recommended Practice for Design and Installation of Offshore Production Platform Piping Systems*, 1991.
- [26] F. Sani, S. Nestic, F. Esaklul and S. Huizinga, *Review of the API RP 14E erosional velocity equation: origin, applications, misuses and limitations*, Nashville: NACE, 2019.
- [27] DNV, *DNVGL-RP-O501 Managing sand production and erosion*, Det Norske Veritas, 2011.
- [28] Ministerie van Economische Zaken, *Ministeriële Regeling Gaskwaliteit* <https://wetten.overheid.nl/BWBR0035367/2019-01-01>, Den Haag: Overheid.nl, 2019.